Modeling Freshwater Inflows and Salinity in the Loxahatchee River and Estuary

Yongshan Wan and Gordon Hu

SUMMARY

This appendix describes the hydrologic and salinity models used in the Northwest Fork of the Loxahatchee River restoration alternative evaluations. The Loxahatchee Watershed (WaSh) model was developed to simulate freshwater flow from each of the tributaries into the Northwest Fork. The WaSh model is based on restructuring HSPF (Hydrologic Simulation Program – Fortran) into a cell-based system with the addition of a groundwater model and a full dynamic channel routing model (Wan et al., 2003). The model is capable of simulating surface water and groundwater hydrology in watersheds with high groundwater tables and dense drainage canal networks. Using long-term flow data collected at S-46, Lainhart Dam, Cypress Creek, Hobe Grove Ditch, and Kitching Creek, the WaSh model was calibrated and validated. The daily flow outputs from the 39-year simulation (1965–2003) provide the basis for the base condition and flow restoration scenarios of the Northwest Fork ecosystem restoration.

The Loxahatchee River Hydrodynamics/Salinity (RMA) model was developed to simulate the influence of freshwater flows on salinity conditions in the Loxahatchee River and Estuary. The RMA model is based on the RMA-2 and RMA-4 and was calibrated against field data from five locations and provided salinity predictions for many other sites where field data are not available. Tide/salinity data collected since 2002 have provided a field database for the investigation of the impact of freshwater inflow on the salinity regime in the Northwest Fork.

To perform long-term predictions of daily salinity, a Long-Term Salinity Management Model (LSMM) was developed to predict salinity and calculate several other performance parameters under various ecosystem restoration scenarios. Field data, regression analyses, and results from multi-dimensional hydrodynamic computer models were integrated into the LSMM as a system simulation and management tool. This salinity management model contains several functions such as the calculation of additional freshwater demand for salinity management and the nutrient loading that would occur under various restoration scenarios.

INTRODUCTION

The Loxahatchee River and Estuary, containing a federally designated Wild and Scenic River system located on the east coast in South Florida, provides habitats supporting a wide spectrum of ecological resources including seagrasses, oysters, saltwater vegetation, and freshwater vegetation. During the past 100 years, the natural hydrologic regime of the Loxahatchee River watershed has been altered by drainage activities associated with urban and agricultural development. Historically, most of the watershed was drained by the Northwest Fork of the Loxahatchee River. Today, much of the watershed has been impacted by the construction of canals and levees for drainage and opening of the Jupiter Inlet. These anthropogenic alterations have resulted in significant encroachment of saltwater-tolerant, mangrove-dominated community

40   into the freshwater, bald cypress-dominated floodplain. Restoration and protection of the
41   Northwest Fork floodplain ecosystem depends largely on providing healthy flow patterns to the
42   river. Development of models capable of predicting long-term freshwater inflow and salinity in
43   the Loxahatchee River and Estuary is critical for the formulation and evaluation of the restoration
44   plan for the Northwest Fork of the Loxahatchee River and Estuary.

45   Over the past several years, the South Florida Water Management District (SFWMD or
46   District) has initiated several projects for data collection and model development. To date, three
47   models have been developed to simulate freshwater inflows and salinity conditions in the
48   Loxahatchee River and Estuary (**Figure 12-1**). These models include a watershed hydrologic
49   model (WaSh) simulating long-term freshwater inflows from all tributaries into the Northwest
50   Fork, a two-dimensional (2-D) estuarine hydrodynamic and salinity model (RMA) that simulates
51   the influence of the freshwater inflows and tide on salinity conditions within the Loxahatchee
52   River and Estuary, and a Long-Term Salinity Management Model (LSMM) that predicts daily
53   salinity conditions according to freshwater inflows from the Loxahatchee River watershed. The
54   LSMM was developed based on the modeling result of the RMA model. During the planning
55   process, a 39-year period of daily freshwater inflow into the river was simulated with the
56   watershed model to ensure that a wide range of climatic conditions was included. Various flow
57   scenarios were proposed and the resulting daily salinity along key assessment locations was
58   simulated with the LSMM. An integrated ecological assessment was carried out to evaluate the
59   ecological benefits with respect to the health of freshwater floodplain vegetation, oysters, and
60   seagrasses in response to these flow scenarios. Such an assessment is critical in selecting
61   restoration alternatives to achieve the comprehensive ecologic benefit of all the ecologic
62   components in the entire system. The purpose of this appendix is to document the calibration and
63   validation results of these models and to provide a description of how these models are used in
64   the evaluation of the Northwest Fork restoration alternatives.
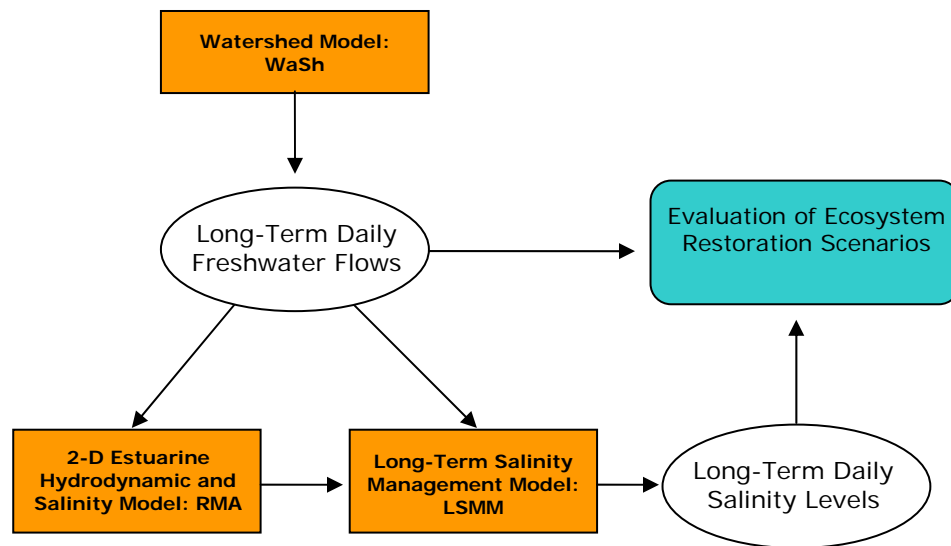

Figure 12-1. The relationship among the three models used to evaluate restoration plan scenarios for the ecosystems in the Loxahatchee River watershed.

65

MODELING FRESHWATER INFLOWS

66

THE WATERSHED MODEL DESCRIPTION

67

68 Freshwater inflows from major tributaries of the Northwest Fork of Loxahatchee River and
69 Estuary are simulated with a Watershed (WaSh) model. This model was developed based on
70 restructuring HSPF (Hydrologic Simulation Program – Fortran, Donigian et al., 1984) into a
71 cell-based system with the addition of a groundwater model and a full dynamic channel routing
72 model (Wan et al., 2003). The WaSh model is capable of simulating hydrology in watersheds
73 with high groundwater tables and dense drainage canal networks, which is typical in South
74 Florida. The model consists of four basic components: (1) a cell-based representation of the
75 watershed basin land surface, (2) a groundwater component that is consistent with the basin cell
76 structure, (3) a surface water drainage system, and (4) water management practices. Key features
77 of the model are surface water and groundwater interactions, irrigation demands, and transfers
78 between elements of the surface water drainage network. For each cell, the model uses an
79 infiltration routine to determine the amount of rainfall that infiltrates into the groundwater,
80 evaporates into the atmosphere, or drains to the surface water system. Currently, the HSPF
81 (Version 12) modules PWATER and IWATER are used for this portion. The infiltrated water is
82 routed to a groundwater model that represents the unconfined aquifer in the watershed. The
83 groundwater model receives the infiltrated water, exchanges groundwater between cells and also
84 exchanges water between surface water flow and groundwater flow. The surface water drainage
85 system consists of a cell-based system and a reach-based system. The reach-based system is
86 typically configured to follow the major canals, streams and rivers and supports branches and
87 common flow structures. The water quality component of WaSh is built on the surface water,
88 groundwater, and channel flow components of the model. The application of the model in the
89 Loxahatchee River watershed focuses on hydrologic simulation. The WaSh model is supported
90 by a Graphic User Interface (GUI) that is developed as an ArcView extension. The GUI handles
91 file management (both on the local platform and on the server), model configuration, execution,
92 and post processing. The WaSh model also supports numerous water management practices such
93 as irrigation, reservoirs, Stormwater Treatment Areas (STAs), and land use changes. Key
94 components of the WaSh model are summarized in **Table 12-1**.

95

96   **Table 12-1.** The watershed (WaSh) model components and functions.

Model Component	Modeling Approach	Functions
Surface Water Flow	PWATER and IWATER of HSPF with PQUAL, SEDMNT, IQUAL, and SOLIDS for water quality	High water table algorithms of HSPF
Groundwater Flow	A new 2-D unconfined groundwater flow model with a prescribed leaching function for water quality constituents	Canal drainage and recharge
Channel Flow	A new 1-D fully dynamic shallow wave model with a scalar mass transport function for water quality	Structures, branching, point sources
Water Management	Reservoirs, Stormwater Treatment Areas, irrigation supply and demands, land use changes	Executed by an ArcView GUI

Model Cell Structure and Cell-Based Routing

97
98   The WaSh model uses a uniform structured grid network. Each cell represents a discrete part
99 of the model domain and has associated physical characteristics such as land use, soil type,
100 ground elevation, impervious area, and a representative ground slope. Hydrological parameters
101 relating runoff, infiltration, and evaporation are specific to these attributes, particularly land use
102 types. If tertiary canals are present in the cell, then the length and width of canals in the cell are
103 computed and added as a cell attribute. Generally, the cell attributes are obtained by combining
104 the cell network with Geographic Information System (GIS) coverage for each of the physical
105 characteristics. For the purpose of routing the simulated daily runoff from each cell, a special cell
106 attribute is assigned to indicate where runoff from that cell is directed. Each cell is labeled as one
107 of three primary types: (1) free cell, (2) canal cell, or (3) reach cell. A free cell represents an area
108 of the basin that does not contain canals. Canal cells are any cells with tertiary canals that are not
109 coincident with the reaches. Reach cells are cells that contain a reach (major canals) in the
110 primary canal system. Some secondary canals can be included in the reach system. These labels
111 are needed to designate the types of surface water and groundwater interactions that may occur
112 for a given cell. **Table 12-2** lists the methods in which water is routed for each type of cell.

113

114

Table 12-2. WaSh water routing operations for each cell type.

115

Cell Type	Flow Routing Operations
Free	Infiltration is directed to cell groundwater
	Surface water is directed to a nearby cell's canals
Canal	Infiltration is directed to cell groundwater
	Surface water is directed to cell canals
	Groundwater can be exchanged with canal surface water
	Surface water can be exchanged between the canal and the reach
Reach	Infiltration is directed to cell groundwater
	Surface water is directed to the cell's reach or nearby cell's canals
	Groundwater can be exchanged with canal or reach surface water
	Reach water can be exchanged with canal water

116

Surface Water and Groundwater Interaction

117
118   The surface water and groundwater is modeled in the same grid network. For each cell, WaSh
119 uses the PWATER and IWATER modules of HSPF (Version 12) to simulate surface water
120 hydrology (**Table 12-1**). A detailed description of these modules is available in the HSPF user's
121 manual (Donigian et al., 1984). Version 12 includes recent model enhancements that simulate
122 irrigation demand, high water tables, and wetland conditions that are common in South Florida
123 (Aqua Terra, 1996; 1998). The HSPF routine is implemented in one-hour time step for 24-hour
124 blocks. Thus, the HSPF-based routine is applied daily for each cell and water balance, consisting
125 of rainfall, evaporation, soil storage, surface runoff and infiltration to groundwater. At the end of
126 each one-day simulation period, the accumulated surface runoff and infiltration are routed to the
127 drainage and groundwater systems, respectively. All HSPF model parameters are calibrated and
128 assigned to each cell based on the land use and soil type characteristics as additional cell
129 attributes.

130   The groundwater module in WaSh is based on the numerical solution of the standard
131   groundwater flow equation for an unconfined aquifer. The model operates on a daily time step,
132   during which it receives infiltrated water, loses water to evaporation, and exchanges water with
133   adjacent cells and with canals. The basic governing equation for the groundwater module is:

134

135
$$\rho \frac{\partial h}{\partial t} = \frac{\partial}{\partial x} K_x (h - h_c) \frac{\partial h}{\partial x} + \frac{\partial}{\partial y} K_y (h - h_c) \frac{\partial h}{\partial y} + S_i - S_e + S_c + S_r \qquad [1]$$

136

137   where h is the groundwater elevation, ρ is the porosity, K_x and K_y are the hydraulic conductivity
138   in the x-, and y- directions, h_c is the aquifer base elevation, and S_i, S_e, S_c, and S_r are source/sink
139   terms representing infiltration, evaporation, exchanges with the canal cells and exchanges with
140   reaches. The governing equation is solved numerically using the basin cell structure. A
141   second-order finite difference approximation is used for the second derivatives, and an explicit
142   backward difference approximation is used for the time derivative. During each time step the
143   right-hand side of the equation is evaluated based on current time level conditions, and the new
144   water elevation is found. By designating the equation parameters and water elevation h for each
145   cell by the indexes $_{i,j}$, and the time level by the index ^{m}, the resulting finite difference equation for
146   each cell is:

$$\frac{1}{\rho_{i,j}} \frac{h_{i,j}^{m+1} - h_{i,j}^m}{\Delta t} = K_x \left[\frac{(\frac{h_{i,j}^m + h_{i+1,j}^m}{2} - h_c)}{\Delta x} \left(\frac{h_{i+1,j}^m - h_{i,j}^m}{\Delta x} \right) - \frac{(\frac{h_{i,j}^m + h_{i-1,j}^m}{2} - h_c)}{\Delta x} \left(\frac{h_{i,j}^m - h_{i-1,j}^m}{\Delta x} \right) \right] +$$

$$[2]$$

$$Ky \left[\frac{(\frac{h_{i,j}^m + h_{i,j+1}^m}{2} - h_c)}{\Delta y} \left(\frac{h_{i,j+1}^m - h_{i,j}^m}{\Delta y} \right) - \frac{(\frac{h_{i,j}^m + h_{i,j-1}^m}{2} - h_c)}{\Delta y} \left(\frac{h_{i,j}^m - h_{i,j-1}^m}{\Delta y} \right) \right] + S_{i_{i,j}}^m - S_{e_{i,j}}^m + S_{c_{i,j}}^m + S_{r_{i,j}}^m$$

147   where Δt is the time step (one day), and Δx and Δy are the grid cell dimensions in each direction.
148   During each time step the right-hand side of the equation is evaluated based on current time level
149   conditions, and the new water elevation is found by solving for $h_{i,j}^{m+1}$. When an active cell is
150   adjacent to the grid boundary or to an inactive cell, a no-flow condition is imposed.

151   Implementation of the groundwater model has required some modification to the PWATER
152   module, primarily to account for evaporation from groundwater and also to link to the irrigation
153   and high water table modules. The original HSPF groundwater algorithm is based on groundwater
154   storage, AGWS. Changes to the storage for each time step are due to infiltration (GWI),
155   evaporation (BASET), and discharge to surface water (AGWO). Infiltration is predicted using
156   subroutines representing the Stanford Watershed Model approach. Evaporation is modeled as a
157   loss term, which is based on a model parameter BASETP. The discharge is based on a rating
158   curve, specified by the model parameters AGWRC and KVARY. This groundwater discharge
159   algorithm in HSPF has been disabled and replaced by the equivalent parameters in WaSh. For
160   each of the cells, two of the source terms on the right hand side of the equation, $S_{i_{i,j}}^m$ and $S_{e_{i,j}}^m$ are
161   set equal to output variables from HSPF PWATER groundwater subroutine related to infiltration
162   (GWI) and evaporation (BASET). The groundwater elevation $h_{i,j}$ replaces the storage variable,
163   AGWS, and when combined with the two source terms, represent essentially the same processes

164   as AGWO in HSPF. However, this modification provides a process-based approach to represent
165   surface water and groundwater interactions when compared with the rating curve-based
166   groundwater discharge approach in HSPF. For example, the source/sink terms for a canal/reach
167   cell are now defined as:

168

169
$$S_{c_{i,j}}^{m} = \frac{\Delta H \, C_c}{A}$$
[3]

170

171
$$S_{r_{i,j}}^{m} = \frac{\Delta H \, C_r}{A}$$
[4]

172

173   where ΔH is the difference in groundwater elevation and canal or reach surface water elevation,
174   which are dynamically tracked in WaSh, A is the cell area, and C_c and C_r are the conductance of
175   canal or reach, respectively. The conductance is physically related to the hydraulic conductivity
176   of the stream bed material and the length and width of the canal. In the Loxahatchee River
177   watershed, the hydraulic conductivity of the deep canals (reaches) and shallow canals is different.
178   The hydraulic conductivity and canal dimension are provided as input data for each cell according
179   to the basin hydrography and land use.

Irrigation Demand and High Water Table Conditions

181   The WaSh groundwater module has also been developed to interact with the irrigation
182   module and the high water table module of the HSPF. WaSh simulates the irrigation demand by
183   monitoring the moisture in the upper and lower soil zones and generating a demand for water
184   based on the existing moisture relative to the desired moisture level that is specified by the user.
185   After the irrigation demand is calculated, the algorithm tries to meet the demand by supplying
186   water from a number of sources. Groundwater can serve as both an irrigation source and an
187   irrigation sink (receptor) in the HSPF irrigation algorithm. In each case, the amount of water
188   demanded from, or applied to, the groundwater is extracted or added to the cell's groundwater
189   volume. At the beginning of each day, the irrigation demand is calculated and if groundwater is
190   affected, then the groundwater elevation $h_{i,j}$ is adjusted according to the following equation:

$$h_{i,\,j} = h_{i,\,j} + \Delta V / \rho$$
[5]

191

192   where ΔV is the volume (expressed as depth) of groundwater irrigation demand or application for
193   the cell calculated by the HSPF irrigation module, and ρ is the aquifer porosity as defined
194   previously in Equation [1].

195   The high water table module in the HSPF requires certain vertically referenced parameters
196   and variables to allow for exchange of water between storage components when the groundwater
197   level interferes with the upper and lower zone storage (UZS and LZS). For applications in WaSh,
198   the vertical referencing is already completed, as the surface elevation (a cell attribute) and the
199   groundwater elevation h are all referenced to the same datum. Thus, the only required
200   modification is to provide these two variables to the high water table algorithms. The HSPF high
201   water table algorithm then calculates the exchange between the storage zones and the
202   groundwater. The groundwater elevation is updated with Equation [5], where ΔV now represents
203   the exchange between the upper and lower storage zones.

204   ## Drainage Canal Network and Canal Routing

205   The surface water drainage canal network is modeled implicitly in the cell-based system and
206   explicitly in the reach-based system. The major channels are simulated in the reach-based system
207   which consists of a series of reaches and nodes. This drainage system is separated from the cell
208   system, but its elements (reaches and nodes) overlay the cell network and coincide with a subset
209   of the cells. This system is typically configured to follow the major canals, streams, and rivers in
210   the basin. The small or tertiary canals are represented in the cell-based system. These canals
211   receive surface and subsurface runoff from the adjacent cells and exchange water with
212   neighboring canal cells.

213   Flow through the reach-based systems is modeled using the continuity equation, Equation [6],
214   and the depth- and width-averaged shallow water wave equation, Equation [7]. The governing
215   equations are:

$$\frac{\partial wh}{\partial t} = \frac{\partial q}{\partial s} + Q_e \qquad\qquad [6]$$

$$\frac{\partial q}{\partial t} + \frac{\partial uq}{\partial s} + \frac{gw}{2}\frac{\partial h^2}{\partial s} = -w\,\tau_b - gwh\,\frac{\partial \eta}{\partial s} \qquad\qquad [7]$$

216

217   where q is the flow, u is the width- and depth-average flow velocity, g is the acceleration due to
218   gravity, w is the canal width, h is the water depth (referenced to the canal bed), η is the bed
219   elevation, t is time and s is distance along the canal. The bottom stress τ_b is based on a
220   Manning's n formulation. Boundary conditions can be one of two types: a specified flow or a
221   specified water elevation. Specified flow conditions are typically used when a flow structure
222   controls the flow out of the system. The water elevation (or head) condition is used when the
223   system drains unobstructed into a receiving water body. The governing equations are solved using
224   a finite volume procedure, with the reach and node system for a single branch equivalent to a
225   finite volume staggered grid approach.

226   The source term Q_e in the continuity equation, Equation [6], consists of point sources or
227   sinks, exchange with groundwater, and exchange with canals from the cell-based system. The
228   units for the source term are flow per unit length of channel. The general form for the source term
229   can be expressed as:

$$Q_e = Q_{kp} + Q_{ki} + Q_{r,gw} \qquad\qquad [8]$$

230

231   where Q_{kp} are external sources or sinks (user specified time series), $Q_{r,gw}$ is the exchange with the
232   groundwater and is equal to S_r, the exchange calculated in the groundwater model, Equation [1],
233   and Q_{ki} is the exchange with the canal cells where the tertiary canals are connected with the reach.

234   When the reach-based system contains branches, the flow in each branch is determined
235   independently. The method for estimating the flow between branches depends on whether the
236   flow is natural at the connection or whether a structure exists. When a structure is present at the
237   branch connections, the flow is determined using a rating curve specific to the structure. Since the
238   flow can be bi-directional, the flow direction for the time step is first determined from the water
239   elevations in the reaches at the branch juncture. The water elevations for headwater and tailwater

240 are then assigned appropriately and the rating curve is used to calculate the flow. It is noted that
241 structures can also occur at any node along the reach node system. When a structure is present,
242 the flow at that node is determined at the beginning of the time step using the structure flow
243 formulas and its value replaces the momentum equation for that node. When no structures are
244 present at the branch connections, the flow is solved using the shallow water wave equation,
245 Equation [7], and the continuity equation, Equation [6]. The two equations are solved explicitly
246 for the flow between branches using the two reaches that connect the branches. The calculated
247 flow in the 'local' explicit solution is then used as a boundary condition for the implicit solution
248 for the upstream branch and as a source to the downstream reach.

249 Flow in the cell-based canal system (i.e., the tertiary canals) is represented in the
250 WaSh model using the same governing equations and numerical scheme as used for the
251 reach-based system. To implement this approach, the cell-based canal parameters are first
252 mapped into a 'local' branch and reach network. When this mapping is completed, the solution
253 algorithm for the reach system can be applied to the local system with only minor modifications
254 to the downstream boundary condition and the source terms. The source term in the cell canal
255 would then include surface runoff simulated with HSPF routines.

256 The tertiary canals are characterized by the total length LC of these canals within the cell, the
257 average canal width w_c, the average canal bottom elevation, and a critical or 'design' water depth.
258 These parameters are attributes of the cell. They can be obtained by mapping GIS hydrologic data
259 onto the basin grid and then specifying widths, bottom elevations and critical depths based on the
260 cell land use. The surface water elevation is the dependent variable in the system. In order to map
261 these parameters into a branched network, each cell's canals are designated as a single reach. The
262 reach parameters for the cell are determined as follows:

263

264   If the total canal length L is less than the cell length LC, then:

265

266 $$\Delta s = L, \quad and \ w = w_c \qquad\qquad [9]$$

267

268 If the total canal length L is greater than the cell length LC, then:

269

270 $$\Delta s = LC, \quad and \ w = w_c * \frac{L}{LC} \qquad\qquad [10]$$
271

272

273 After the cell-based canal parameters are transformed into reach parameters, the connectivity
274 of the branch network is determined. The connectivity of the cells is used directly to establish
275 branches and the assignments of reaches within each branch. The canal-to-canal flow is generally
276 towards the reaches, but the instantaneous flow is determined by the difference in relative surface
277 water elevations between hydraulically connected canal cells. When canal cells exist in cells with
278 reaches, the canals are assumed to be hydraulically connected to the reach via a structure. It is in
279 these cells that water can flow between the canals and reaches. Between the reaches and tertiary
280 canals, the flow is assumed to be controlled by pumps. The pumping capacity is derived from
281 land use types, representing the design (or estimated) drainage capacities for the canal systems
282 associated with each land use. The drainage capacities of the major land use types are the key
283 parameters for calibrating the magnitude of peak flow during a high magnitude and low
284 frequency event.

285   **IMPLEMENTING THE WASH MODEL**

286   **Watershed Delineation**

287   The Loxahatchee River watershed is located within northern Palm Beach and southern Martin
288   counties and currently drains an area of approximately 240 square miles. Much of the watershed
289   remains as undeveloped sloughs and wetlands. In the upper portion of the watershed, nearly half
290   of the drainage basin is comprised of wetlands. Agriculture and forested uplands in the northern
291   area of the basin comprise one quarter of the watershed. The remaining quarter of the watershed
292   consists of developed urban areas.

293   The Loxahatchee River watershed was delineated into 12 drainage basins based on local
294   hydrology, land use, topography, detailed aerial photography, and field observations. These
295   basins represent the same areas as the seven sub-basins described in the Loxahatchee River
296   Watershed Action Plan (FDEP, 1998); four of the FDEP sub-basins have been subdivided into
297   separate basins to reflect the specific needs of modeling. The basins vary in size from 5 to
298   100 square miles, and they provide flow to the three forks of the Loxahatchee River
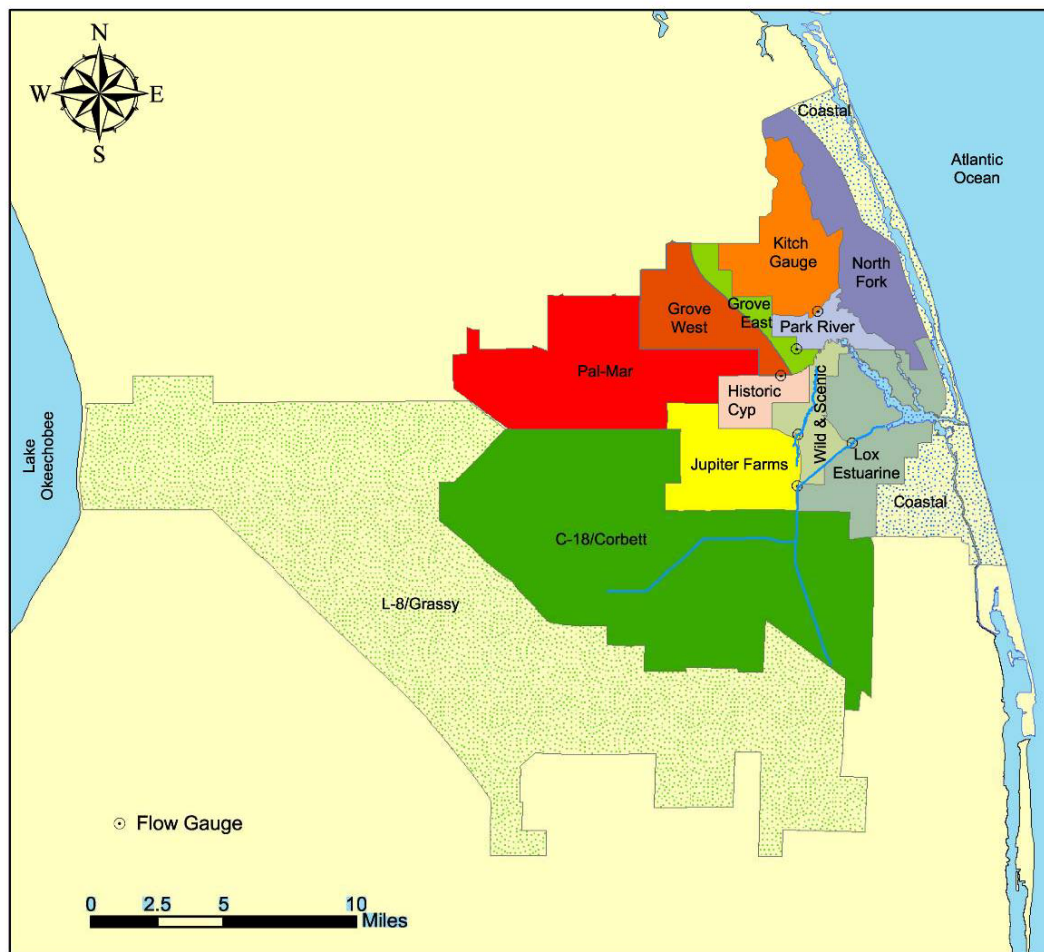299   (**Figure 12-2**).

Figure 12-2. Major drainage basins in the Loxahatchee River watershed.

300   The 1995 land use for these basins has been modified to include changes in the developed areas
301   for the year 2000. For purposes of this plan, the 133 land use codes were reduced to six land use
302   categories: citrus and vegetables, forest, marsh wetland, other wetland, urban, and other land.
303   **Table 12-3** shows the breakdown of land use by basin for the Loxahatchee River watershed.

304

305   **Table 12-3.** Loxahatchee River watershed 1995 land use by basin; developed
306   areas updated for the year 2000.

Basin	Land Use (acres)						Total Area by Basin	
	Citrus & Vegetables	Forest	Marsh Wetland	Other Wetland	Urban	Other Land	Acres	Square Miles
1. Kitch Gauge	16	876	4,954	1,010	309	3,177	**10,342**	**16.2**
2. North Fork	0	95	8,238	735	1,774	156	**10,999**	**17.2**
3. Park River	14	60	2,483	47	31	408	**3,044**	**4.8**
4. Lox Estuarine	591	305	1,155	617	10,536	34	**13,237**	**20.7**
5. C-18/Corbett	1,821	822	43,591	4,749	9,199	3,312	**63,494**	**99.5**
6. Historic Cypress Creek	340	12	2,993	132	85	20	**3,581**	**5.6**
7. Pal-Mar	266	88	19,477	555	1,672	605	**22,663**	**35.4**
8. Grove West	4,107	168	2,878	86	54	906	**8,199**	**12.8**
9. Grove East	1,709	143	397	105	309	345	**3,010**	**4.7**
10. Jupiter Farms	8	89	494	168	9,359	128	**10,246**	**16.0**
11. Wild & Scenic	752	142	2,562	220	278	392	**4,345**	**6.8**
12. Coastal	0	2,190	2,212	2,180	8,899	391	**15,872**	**24.9**
Total Area by Land Use — Acres	**9,624**	**4,990**	**91,434**	**10,603**	**42,505**	**9,874**	**169,031**	
Total Area by Land Use — Square Miles	**15.1**	**7.8**	**143.3**	**16.6**	**66.6**	**15.5**	**264.9**	

Note: Blue shaded rows are watershed basins that discharge into the Northwest Fork of the Loxahatchee River.

307

308   **Basin 1: Kitch Gauge.** This basin contains the 16.2-square-mile area that contributes water
309   to the USGS Kitching Creek flow gauge in Jonathan Dickinson State Park. Almost 50 percent
310   (4,654 acres) of this basin is characterized as marsh wetland. Downstream of this basin, Kitching
311   Creek discharges into the Northwest Fork.

312   **Basin 2: North Fork.** This basin contains the 17.2-square-mile area that contributes water to
313   the North Fork of the Loxahatchee River. Approximately 75 percent (8,238 acres) of this basin is
314   marsh wetland. The flow from this basin is not gauged.

315   **Basin 3: Park River.** This basin contains the 4.8-square-mile area that drains to the
316   Northwest Fork of the Loxahatchee River. It includes the portion of land draining to Kitching
317   Creek downstream of the gauge and some smaller tributaries such as Wilson Creek and the creek
318   flowing through the Boy Scout Camp. Approximately 82 percent (2,483 acres) of this basin is
319   marsh wetland. The flow from this basin is not gauged.

320   **Basin 4: Lox Estuarine.** This central drainage basin is a 20.7-square-mile area and is highly
321   developed with urban land uses that contribute significant runoff to the embayment of the
322   Loxahatchee River. Consisting of 20.7 square miles of the watershed, this basin provides aquatic
323   recreational opportunities that sometimes exceed the river's carrying capacity on weekends and

324   holidays. Runoff and groundwater from this basin discharge to brackish waters of the estuary.
325   Approximately 80 percent (10,536 acres) of this basin is urban. The flow from this basin is not
326   gauged.

327   **Basin 5: C-18/Corbett.** With 100 square miles, this is the largest basin in the Loxahatchee
328   River watershed. Much of the land in this basin encompasses the southwestern portion of the
329   watershed, and it is publicly owned and protected. This basin includes the remnants of the
330   Hungryland and Loxahatchee sloughs, which historically fed the Northwest Fork of the
331   Loxahatchee River. Historically, the Loxahatchee Slough extended south into the area currently
332   known as the Grassy Waters Preserve (West Palm Beach Water Catchment Area), which is the
333   present source of drinking water for the City of West Palm Beach. Water from this basin
334   discharges to the C-18 canal and is either discharged into the Southwest Fork of the Loxahatchee
335   River through the S-46 structure or directed through the G-92 structure to the upper end of
336   Northwest Fork of the Loxahatchee River. Approximately 69 percent (43,591 acres) of this basin
337   is marsh wetland. Flow gauges are located at the G-92 and the S-46 structures.

338   **Basin 6: Historic Cypress Creek.** Cypress Creek is a 5.6-square-mile basin that drains to
339   Cypress Creek just downstream of the Cypress Creek flow gauge. The majority of this basin has
340   recently been purchased by state and local governments for restoration and preservation. Water
341   from this basin flows into Cypress Creek and discharges at the upper end of the Northwest Fork
342   near River Mile (RM) 10.3. Approximately 84 percent (2,993 acres) of this basin is marsh
343   wetland. The flow from this basin is not gauged.

344   **Basin 7: Pal-Mar.** Pal-Mar is a 35.4-square-mile basin that drains a sizable wetland located
345   along the western edge of the watershed and is one of the major tributaries to the Northwest Fork
346   of the Loxahatchee River. Most of these wetlands remain intact; however, the eastern flow-ways
347   leading to Cypress Creek have been disturbed by rural development. Approximately 86 percent
348   (19,477 acres) of this basin is marsh wetland. Water from this basin flows into Cypress Creek
349   upstream of the Cypress Creek flow gauge and discharges at the upper end of the Northwest Fork
350   near RM 10.3.

351   **Basin 8: Grove West.** The predominant land use in this 12.8-square-mile basin is citrus.
352   Although the hydrology in this basin was altered to support agriculture, wildlife utilization is
353   relatively good, and the land provides a valuable greenway link between large natural areas
354   within the watershed. Approximately 50 percent (4,107 acres) of this basin is used for vegetables
355   and citrus. Water from this basin flows into Cypress Creek upstream of the Cypress Creek flow
356   gauge and discharges at the upper end of the Northwest Fork.

357   **Basin 9: Grove East.** The predominant land use in this 4.7-square-mile basin is citrus.
358   Although the hydrology in this basin was altered to support agriculture, wildlife utilization is
359   relatively good, and the land provides a valuable greenway link between large natural areas
360   within the watershed. Approximately 57 percent (1,709 acres) of this basin is used for vegetables
361   and citrus. Water from this basin flows into Hobe Grove Ditch (RM 9.07) and Moonshine Creek
362   (RM 10.0), both of which discharge into the Northwest Fork near RM 9.0.

363   **Basin 10: Jupiter Farms.** This 16-square-mile basin supports substantial rural residential
364   development known as Jupiter Farms. The South Indian River Water Control District (SIRWCD)
365   manages a stormwater management system of canals to serve this area. Water quality and
366   saltwater intrusion in the Northwest Fork are concerns in this basin (FDEP, 1998). Water from
367   this basin discharges into the SIRWCD C-14 canal, which flows over Lainhart Dam feeding the
368   upper end of the Northwest Fork. The C-18 canal is connected to this basin by the G-92 structure,
369   which also provides periodic flows of water over the Lainhart Dam from the C-18 canal.
370   Approximately 91 percent (9,359 acres) of this basin is urban land. There is a flow gauge at both
371   G-92 and Lainhart Dam.

372   **Basin 11: Wild and Scenic.** This 6.8-square-mile area basin contains the "Wild and Scenic"
373   Northwest Fork of the Loxahatchee River and the northern portion of Riverbend Park.
374   Approximately 59 percent (2,562 acres) of this basin is marsh wetland. The flow from this basin
375   is not gauged.

376   **Basin 12: Coastal.** The coastal basin contains the 34-square-mile area that drains to the
377   Atlantic Ocean or the Intracoastal Waterway and out the Jupiter Inlet. This basin has been
378   developed for maximum urban residential, commercial, and recreational use. Very few small and
379   isolated natural areas remain. Most of the surface water and groundwater from this basin
380   discharge to marine waters rather than toward the freshwater portion of the Northwest Fork. The
381   flow from this basin is not gauged.

382   **Adjacent Basin: L-8/Grassy.** This 192.5-square-mile basin is not considered part of the
383   Loxahatchee River watershed. However, this basin has several outflow locations, one of which is
384   to the C-18/Corbett Basin. Thus, the inter-basin transfers of waters from Grassy Waters to the
385   C-18 canal are considered in this plan. There are no flow gauges at this inter-basin location.

Model Setup

387   The WaSh model was implemented into four regions of the Loxahatchee River watershed
388   (**Figure 12-3**). These regions include all of the major drainage basins except the Coastal Basin.
389   The JDSP region (A) includes the North Fork, Kitch Gauge, Park River, and the Loxahatchee
390   Estuary basins. The Pal-Mar and Grove region (B) includes the Pal-Mar, Historic Cypress Creek,
391   Grove West, and Grove East basins. The Jupiter Farms region (C) includes the Jupiter Farms and
392   the Wild and Scenic basins. The C-18 region (D) represents the C-18/Corbett Basin and flow
393   diversion from the L-8/Grassy Basin. The cells for each of the regions are shown in **Figure 12-2.**
394   The cell size was 750 ft by 750 ft for the Jupiter Farms region, 1000 ft by 1000 ft for the JDSP
395   region and Pal-Mal/Grove region, and 1500 ft by 1500 ft for the C-18 region.

396   Input data required to generate the model grid include primary and secondary basin
397   coverages, polygon features with basin name attributes, hydrography including streams and
398   canals as line or polyline features, the 2000 base land use coverage, soil coverage, and land
399   surface elevation. The land surface contour was resampled (100-foot intervals) based on 5 ft by
400   5 ft Light Detection and Ranging (LIDAR) data to get a smooth land surface profile and to
401   remove data artifacts. For limited areas where LIDAR data are not available, the 1-foot contour
402   was used. Using the ArcView GUI, these coverages are overlaid to get an aerial extent of the
403   model domain along with cell attributes of land use type, soil, canal length and width, and
404   elevation.

405   When creating the primary reaches for the basins, the hydrography theme is overlaid on the
406   grid and those grid cells intersecting with polylines of the hydrography theme are classified as
407   canal cells. The canal length in a grid cell is calculated with all the intersecting canal segments
408   inside a grid cell. Reach cells are created by digitizing major river segments and canals starting
409   from the basin outlet. After digitizing, the length of a reach, which is typically the grid cell size, is
410   specified to allow for redistribution of the nodes along the reach network. Each of the reach
411   segments has a reach ID along with the width and bottom elevation assigned according to the
412   cross-section of the major canal and river segment. In **Figure 12-3**, the cells are colored coded to
413   represent canal cells (turquoise), reach cells (pink), and free cells (light green). The surface
414   elevation of cells is used to create flow paths. In general, flow in free cells is routed to the nearest
415   canal or reach cell (**Figure 12-3**, Region B). A no flow boundary condition is imposed along the
416   boundary cells.

417
418
419
420
421
422
423
424
425
426
427
428
429
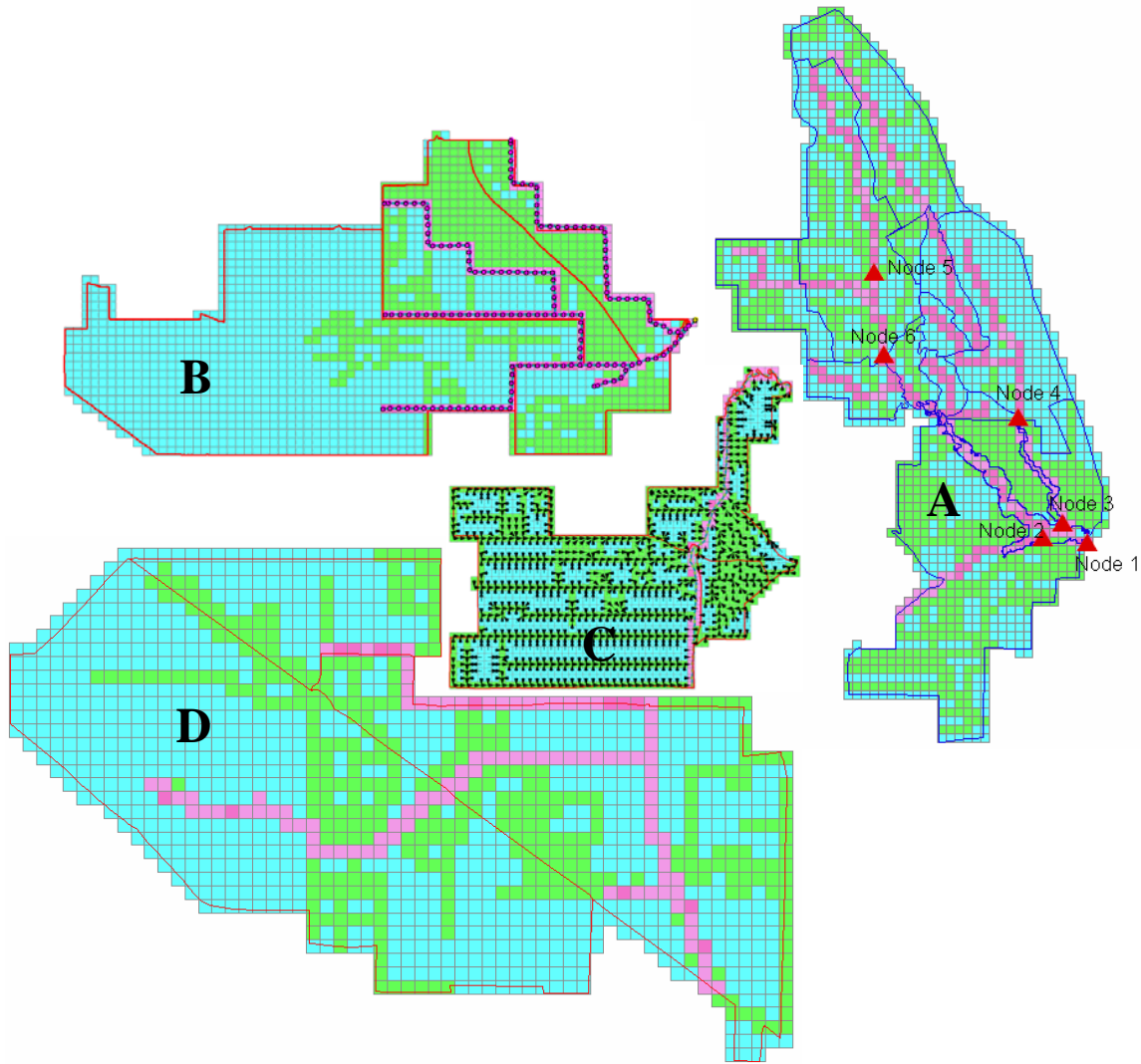430
431
432
433
434
435
436
437
438

Figure 12-3. The Loxahatchee WaSh model grids: (A) JDSP model,
(B) Pal-Mar-Grove model, (C) Jupiter Farm model, and (D) C-18 model.
Free cells, canal cells, and reach cells are color coded turquoise, light
green, and pink, respectively. In Region A, the blue line represents the
model boundary, and the nodes represent examples of possible model
output locations. In Region B, the nodes are show in the reach system.
In Region C, flow routing directions are shown with arrows.

Each of the cells is linked with a Master Lookup Database consisting of HSPF parameters,
evapotranspiration (ET) coefficients, canal parameters, and aquifer properties. Based on the grid
cell attribute, this master database is queried to populate the respective parameters for each cell in
the grid. Some of the model parameters can be changed during the model calibration process.

The other important input data required by the model are rainfall and ET. These data were
obtained from the District's South Florida Water Management Model (SFWMM) for the period
from 1965–2000. The data set was extended to March 2004 with available rainfall and ET data
stored in the District's DBHYDRO database in the model area. Daily rainfall is disaggregated
into hourly rainfall based on an analysis of available hourly rainfall distribution in South Florida.

454   **Model Calibration and Validation**

455   The Loxahatchee WaSh model has been calibrated with five flow monitoring stations
456   (**Figure 12-4**). Flow data collected at the G-92 structure are not used since it was found that the
457   data are likely not accurate. The Kitching Creek station started to collect data in the early 1980s.
458   The data are not continuous until 1990, and thus only the data collected after 1990 are used for
459   calibration and validation of the JDSP model. The Hobe Grove and the Cypress Creek stations
460   have been collecting data since 1980; however, there are significant periods of time when data
461   were not collected or are missing. Data collected from the flow stations at S-46 and Lainhart Dam
462   have the longest record. Only the data collected after 1987 were used for WaSh model calibration
463   and validation due to structure changes of G-92. All the collected flow data were evaluated for
464   their validity before being used for model calibration and validation. In addition, water level data
465   collected in a groundwater well (PB-689) were used. The well is located in the C-18/Corbett
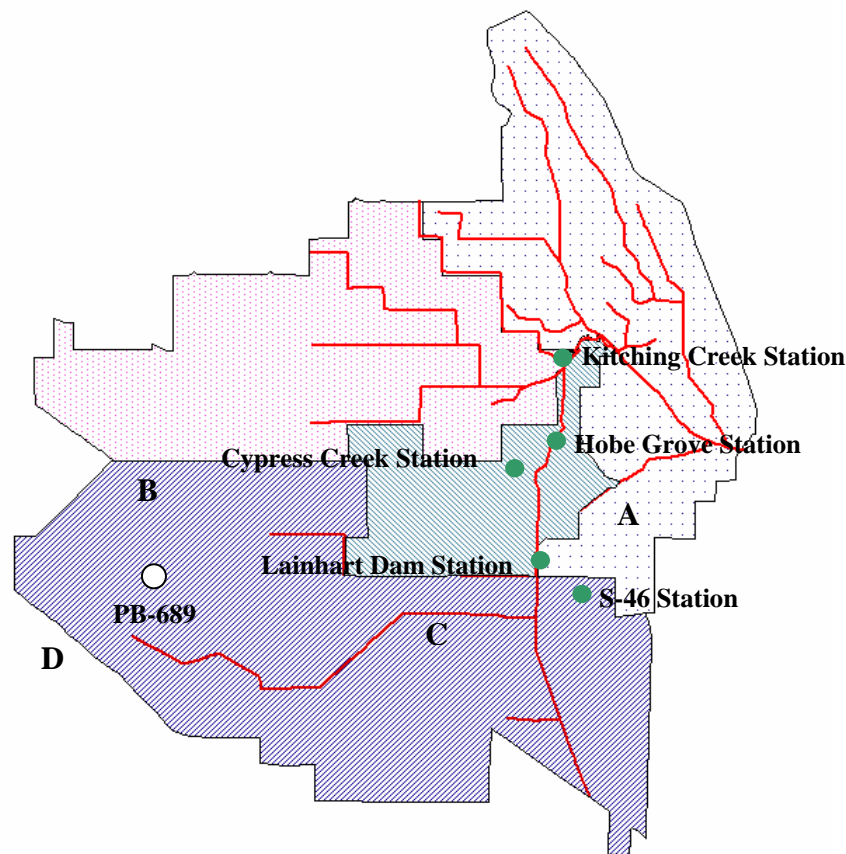466   basin where the land use is dominated by wetland.

Figure 12-4. Flow (green dots) and groundwater (white dot) monitoring stations
in the Loxahatchee River watershed for WaSh model calibration arrows.

467   Model calibration involves conducting a model simulation of each region for the period of
468 record (POR) and comparing the simulated flow with the observed flow. The model parameters
469 are then adjusted in subsequent simulations to improve the shape of simulated flow time-series
470 until the model output meets the performance criteria. In general, the hydrological calibration is
471 conducted in two main steps:

472 1. Macro Scale: Adjust hydrological parameters to obtain the long-term basin water budget.

473 2. Micro Scale: Fine tune model parameters to get the best match between observed and
474   simulated flow. At this stage, the shape of the hydrograph with respect to peak and base flow
475   is adjusted. Groundwater levels were also checked with data from observation wells.

476   In the first step, the long-term water budget is used to ensure that the model calibrations are
477 not biased for one type of climatic condition. Another component of the water budget calibration
478 is verifying that the fractions of groundwater and surface water contribution to runoff properly
479 reflect the partitioning between surface runoff and subsurface runoff. For this component of the
480 simulation, the average annual water budget for each of the land uses as well as for the entire
481 watershed were used to make decisions to adjust parameters. An initial run of the model was
482 made using model parameters that were calibrated in the St. Lucie Estuary watershed (Wan et al.,
483 2003). The most sensitive model parameters in completing the water budget calibrations are
484 evaporation coefficients for individual months and infiltration parameters of the HSPF. An
485 example of the water budget is provided in **Table 12-4** for the Pal-Mar and Grove regions. The
486 water budget is partitioned into the Pal-Mar and historic Cypress Creek basins, which consist
487 mostly of wetland and forest, and the Grove West and Grove East basins, which consist mostly of
488 irrigated citrus groves. Citrus irrigation significantly increases the runoff from a water budget
489 perspective.

490

491

Table 12-4. Average annual water budget (inches) for the Pal-Mar and
492   Grove regions.

493

Basins	Rainfall	Irrigation	ET	Runoff		Storage
				Surface	Subsurface	
Pal-Mar & Historic Cypress Creek	61.2	--	44.9	13.6	2.6	1.7
Grove West & Grove East	61.2	8.2	40.2	16.9	11.9	0.2

494   Once the long-term calibration is completed, the next step is to validate the model by
495   matching the simulated daily flow hydrograph to the measured daily flow values recorded for
496   each of the flow stations. The more significant parameters to be calibrated during this step
497   includes the groundwater cell conductance parameters that control the rate at which groundwater
498   flows to the canals, the irrigation parameters, and the canal pumping parameters that control the
499   rate at which tertiary canals flow to primary reaches. To a lesser degree, the length-scale
500   parameter associated with surface drainage (LSUR) has an affect on the shape of the
501   hydrographs. Reducing the LSUR increases runoff and decreases infiltration. The model
502   validation process is similar to the calibration process, except that a different POR is used for the
503   relevant input data. The model parameters are kept constant. Model validation is considered
504   complete if the simulation meets the performance criteria. Otherwise, the model is
505   recalibrated and validated.

506   Model calibration and validation performance are evaluated with two of three criteria
507   recommended by the ASCE Task Committee on Definition of Criteria for Evaluation of
508   Watershed Models (1993): the deviation of volume, the Nash-Sutcliffe coefficient, and the
509   coefficient of daily gain. The coefficient of gain from the daily mean is not used because of its
510   similarities with the Nash-Sutcliffe coefficient in this particular case. Instead, the coefficient of
511   determination (R^2) is calculated as part of the hydrologic analysis.

512   The deviation of volume, DV, quantifies the difference in observed and predicted water
513   volumes and is calculated:

514
$$DV = \frac{\sum\limits_{i=1}^{n}(Vm - Vs)}{\sum\limits_{i=1}^{n}Vm} \times 100\% \qquad [11]$$

515

516   where DV is the deviation of volume (%), Vm is the measured water yield for the period of
517   comparison, and Vs is the modeled water yield for the period of comparison.

518   The Nash-Sutcliffe coefficient, NS, measures how well the daily simulated flow corresponds
519   with the measured flow. This coefficient is calculated:

520

521
$$NS = 1 - \frac{\sum\limits_{i=1}^{n}(Qm - Qs)^2}{\sum\limits_{i=1}^{n}(Qm - Q)^2} \qquad [12]$$

522

523   where Qm is the measured daily discharge, Qs is the simulated daily discharge, and Q is the
524   average measured daily discharge. A Nash-Sutcliffe value of 1.0 indicates a perfect fit, while a
525   value of 0 indicates that the model is predicting no better than the average of the observed data.

526   The model calibration and validation performance results are summarized in **Table 12-5**.
527   Note that during the period of model calibration or validation, those days with missing or
528   problematic data were excluded, so the count of days indicates the number of days with valid
529   flow data. In general, the model simulates daily flow reasonably well with almost all R^2 and NS
530   values about 0.5 for both calibration and validation analyses. Except for the Hobe Grove station,
531   the DV ranged from −0.83 to 8.5 percent for calibration and −2.87 to 12.5 percent for validation.

532
Table 12-5. WaSh model calibration and validation performance results.
533

Monitoring Station	S-46	Lainhart Dam	Cypress Creek Station	Hobe Grove Station	Kitching Creek Station
Calibration Results					
Period	1987–1996	1987–1996	1980–1986	1981–1985	1990–1996
Number of days	3193	3193	1680	1058	2192
DV (%)	−1.78	−0.83	−7.50	−14.67	0.21
NS	0.69	0.47	0.43	0.08	0.51
R^2	0.71	0.53	0.53	0.54	0.51
Validation Results					
Period	1997–2004	1997–2004	1987–1990	1987–1989	1997–2000
Number of days	2587	2587	990	687	1461
DV (%)	12.52	9.43	−2.87	10.66	9.09
NS	0.71	0.56	0.61	0.27	0.54
R^2	0.73	0.32	0.72	0.63	0.57

534
535

536   To aid in the evaluation of model calibration and validation performance, three types of plots
537 are prepared:

538 1. Daily flow distribution: Plot of the distribution of the measured and modeled daily flow to
539   visually examine the overall model performance. Particular attentions are paid to the low
540   flow regime.

541 2. Double mass curve: To compare the measured and modeled daily flow in a
542   cumulative manner along with increasing rainfall. This is a visual check of the DV calculated
543   in **Table 12-5**.

544 3. Daily flow time series of modeled flow and observed flow for selected periods.

545

546   **Figure 12-5** includes the three plots for the Lainhart Dam and S-46 stations, which provide
547 the longest period of flow data for model calibration and validation. Panels A and B in
548 **Figure 12-5** compare the frequency distribution of the modeled versus the observed daily flows.
549 A slight high frequency of flow in the range of about 10 cfs is predicted by the model at Lainhart
550 Dam, possibly due to low flow leakage at the structure becoming significant but is not measured.
551 The double mass curves for both stations (**Figure 12-5,** Panels C and D) show consistent model
552 performance when comparing the patterns of the increase of modeled and measured flow with
553 increasing rainfall. At Lainhart Dam, the model over-predicted flow for a 3-month period during
554 the wet season of 1999. This has been attributed partly to the 9 percent of DV in **Table 12-4**.
555 Panels E and F in **Figure 12-5** are the time-series plots of measured flow and modeled flow from
556 2000 through 2003. Overall, the figure shows that the model simulates daily flows over Lainhart
557 Dam and S-46 stations reasonably well.

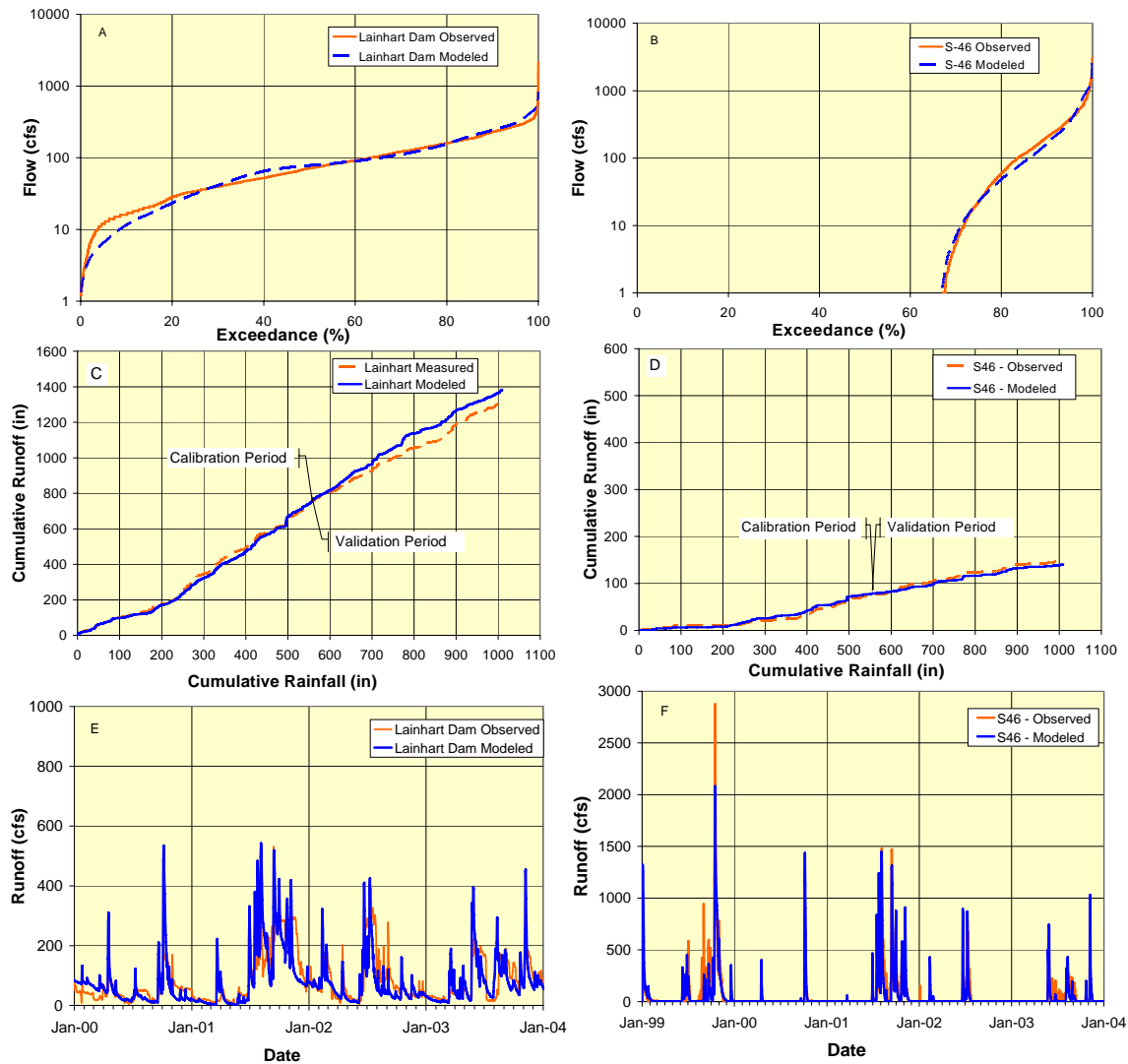**Figure 12-5.** WaSh model calibration and validation plots at Lainhart and S-46 stations (1/1/87–1/31/04): (A) daily flow distribution at Lainhart Dam station, (B) daily flow distribution at S-46 station, (C) double mass curve at Lainhart Dam station, (D) double mass curve at S-46 station, (E) time-series plot at Lainhart Dam station (2000–2004), and (F) time-series plot at S-46 station (1999–2004).

558   Calibration of the C-18 and Jupiter Farms portion of the model is difficult because the Jupiter
559   Farms Basin, the C-18/Corbett Basin, and the Grassy Water Preserve Basin are hydrologically
560   connected. The model represented the G-92 structure by using the 'special structure' option. In its
561   simplest form, the special structure consisted of a weir with a 12-foot elevation located in a reach
562   consistent with its location along the C-18 canal. When the water elevation in the C-18 canal is
563   above 12 feet, the weir structure will allow water from the C-18 canal to flow out of the basin.
564   This discharge was subsequently used as input into the Jupiter Farms Basin as the model
565   boundary condition. The flow rate is determined internally by the model, and is dependent on the
566   prescribed weir configuration and the water elevation in the C-18 canal. The width of the special
567   weir was adjusted in a series of simulations until approximately 50 cfs of water flows during
568   normal operations and a maximum of approximately 400 cfs flows under the flood control mode.

569   Similarly, for the inter-basin transfer of water from the Grassy Waters Preserve (West Palm
570   Beach Water Catchment Area) into the C-18 Canal, a special structure was imposed in a separate
571   model set up for the L-8 Basin to allow for a time series of flow as the boundary condition for the
572   C-18 Basin model. Water flow was based on stage in the Water Catchment Area. According to a
573   water budget model developed for the West Palm Beach Water Catchment Area (Sculley, 1995),
574   an annual contribution of 20,000 ac-ft of water from the Water Catchment Area to the C-18 Basin
575   during April 1992 to March 1995 was used as a target to calibrate the special structure. The
576   time-series plots for Lainhart Dam and S-46 station (**Figure 12-5,** Panels E and F) indicate that
577   the special structures provide a reasonable estimation of inter-basin transfers over the G-92
578   structure and through the existing culverts in Grassy Waters Preserve into the C-18 basin.

579   The Kitching Creek station collects flow from a large area dominated by forest and wetland.
580   **Figure 12-6** presents the performance of the model calibrated and validated at Kitching Creek.
581   Overall, the figure shows that the model is capable of simulating flow fairly well in this area. The
582   daily flow distribution of the modeled flow matches very well with the measured flow. The
583   double mass curves are consistent with 0.21 percent of *DV* for calibration and 9.09 percent for
584   validation shown in **Table 12-4**. However, the time-series plot (**Figure 12-6**, Panel C) did show
585   that in 1998 there were a few significant events that are not predicted by the model. Such
586   deviations are likely related to the quality of rainfall data.

587   The plots for the Cypress Creek and Hobe Grove Ditch stations are shown in **Figure 12-7**.
588   The plots for the Cypress Creek station are consistent with the model calibration and validation
589   performance measures shown in **Table 12-4**. Model calibration and validation at the Hobe Grove
590   Ditch station is not as good as for the Cypress Creek station. This is likely due to the quality of
591   the data collected at the site. The Hobe Grove Ditch dataset is obtained from a stage–flow
592   relationship downstream from several culverts that discharge from Gulf Stream Grove (owned by
593   the District) and the structure owned by the Hobe St. Lucie Water Control District. Measuring
594   flows under these conditions is challenging due to the complexity of the hydrologic connections
595   and grove operations along with slight tidal influence in the downstream area. The stage-flow
596   relationship is not as accurate as other flow gauges in the District. For example, in 1987 the Hobe
597   Grove Ditch station failed to collect accurate data during several significant storm events; these
598   significant events were accurately recorded by the nearby Cypress Creek station (**Figure 12-7**,
599   Panels E and F). Nevertheless, model calibration and validation at the Hobe Grove Ditch station
600   is still considered to be acceptable in light of the poor data quality.
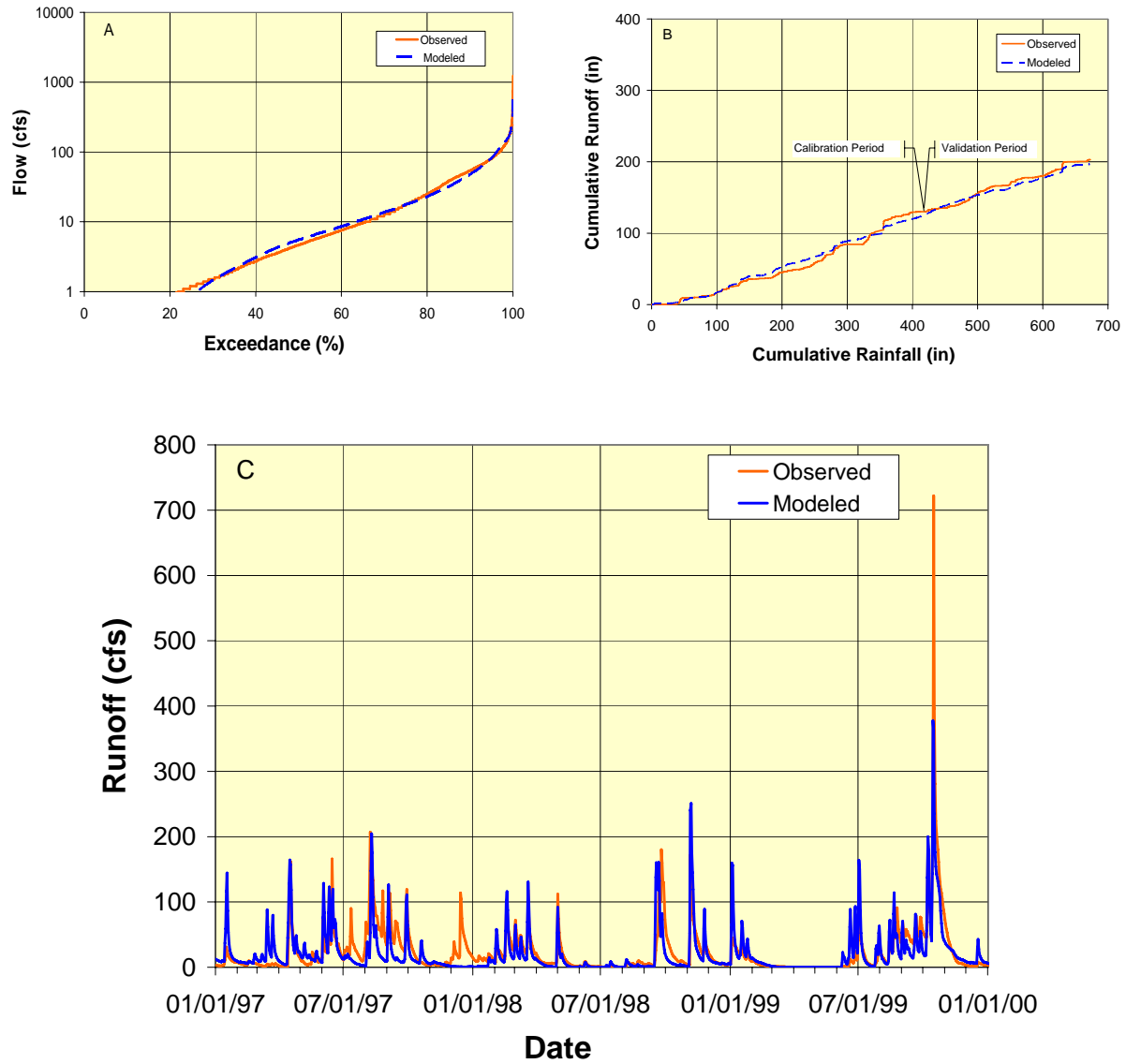
Figure 12-6. WaSh model calibration and validation plots at Kitching Creek station (1990–2000): (A) daily flow distribution, (B) double mass curve, and (C) time-series plot (1997–2000).
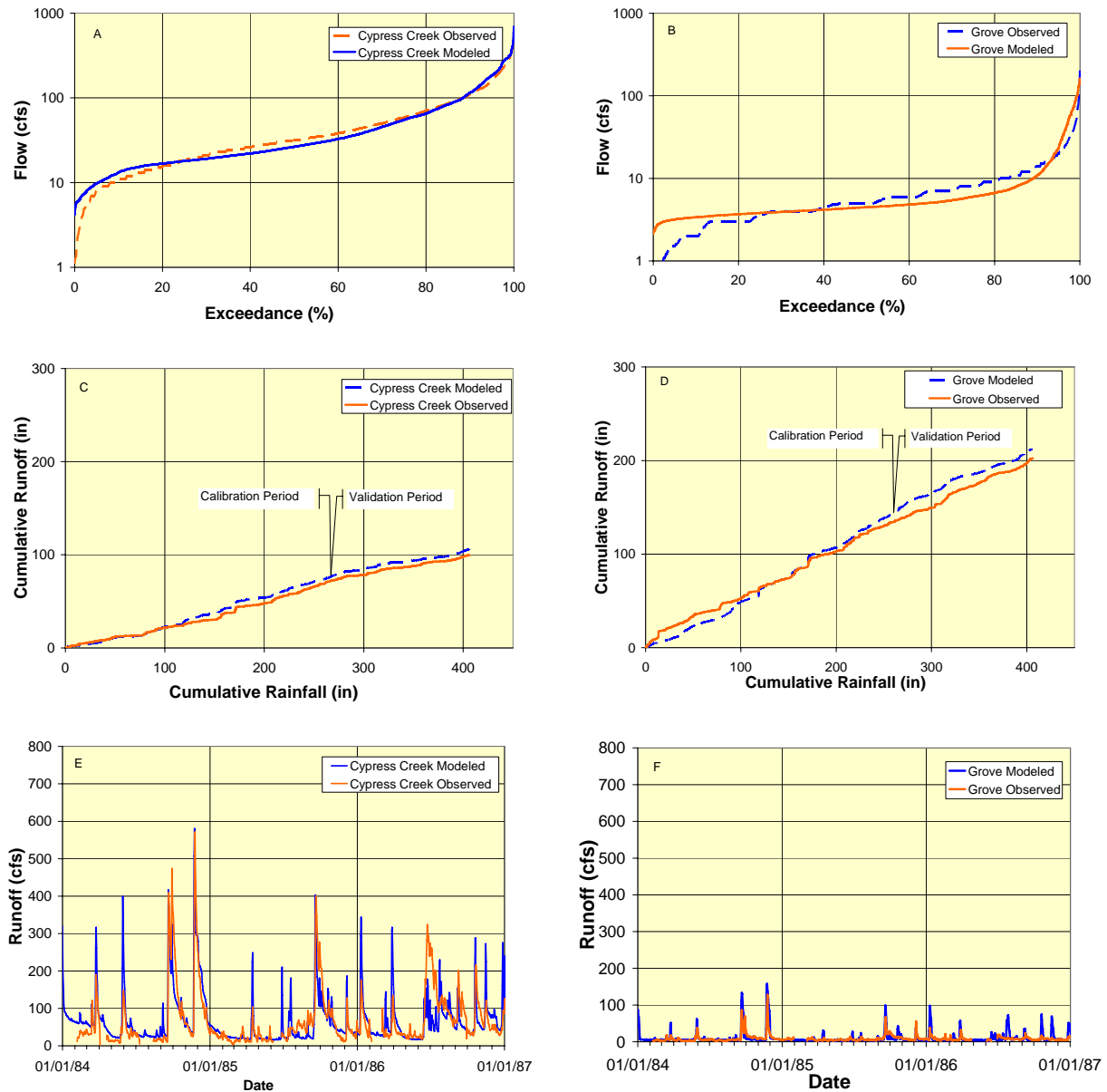
Figure 12-7. Model calibration and validation plots at Cypress Creek and Hobe Grove Ditch Stations (1981–1990): (A) daily flow distribution at Cypress Creek station, (B) daily flow distribution at Hobe Grove Ditch station, (C) double mass curve at Cypress Creek station, (D) double mass curve at Hobe Grove Ditch station, (E) time-series plot at Cypress Creek station (1984–1987), and (F) time-series plot at Hobe Grove Ditch station (1984–1987).

601   The calibration of the groundwater level was conducted in the last step of WaSh model
602   calibration. **Figure 12-8** shows the time series of the observed and modeled water levels at the
603   groundwater monitoring well in the C-18 basin. The cell hydrology simulated by the model is
604   reasonable. Water level predictions could be further refined if the model is to be used for water
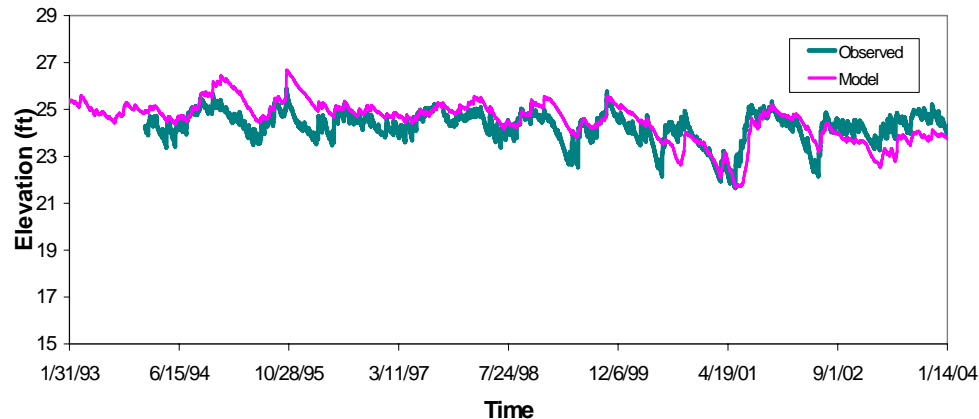605   level evaluations.

606
607   .
608
609   **Figure 12-8.** Observed and modeled water levels at the groundwater
610   monitoring well (PB-689) in the C-18 basin. Land surface elevation
611   for the well is 24.43 feet.
612

WaSh MODEL SIMULATION RESULTS

614   A final long-term simulation for the period from 1965–2003 was conducted after the
615   calibration and validation of the Loxahatchee WaSh model was completed. Daily flows from each
616   of the tributaries and each of the basins were averaged based on the model output of the 39-year
617   simulation. **Table 12-6** is a summary of the data expressed as daily average flows and percentage
618   of contributions from each of the basins (tributaries) into the Loxahatchee River and Estuary and
619   the Northwest Fork. On average, the Northwest Fork receives about 65 percent of total freshwater
620   inflow into the entire Loxahatchee River and Estuary. For total freshwater inflows into Northwest
621   Fork, flow over Lainhart Dam (C-18/Corbett G-92 plus Jupiter Farms) accounts for about
622   45 percent. The next largest contributor is Cypress Creek (32 percent with Pal-Mar and Grove
623   West combined). Kitching Creek at the monitoring station contributes about 8 percent, and Hobe
624   Grove Ditch contributes about 5 percent. The remaining 8 percent is contributed from the areas
625   that are not currently covered by flow monitoring stations. However, the actual freshwater flow
626   contribution varies on a daily basis, depending on the specific hydrologic condition and water
627   management practices. For example, there is little freshwater flow from S-46 during the dry
628   season, whereas a disproportionately large quantity of fresh water is released from S-46 during a
629   flood event.

630

631   **Table 12-6.** Flow contributions from each of the basins and major tributaries into
632   the Northwest Fork and Loxahatchee River and Estuary.

633

Basin	Average Daily Flow (cfs)	Flow Contribution	Northwest Fork Average Daily Flow (cfs)	Northwest Fork Flow Contribution
1. **Kitching Gauge**	17.4	5%	17.4	8%
2. **North Fork**	20.2	6%	--[a]	--[a]
3. **Park River**	5.1	2%	5.1	2%
4. **Lox Estuarine**	14.4	13%	--[a]	--[a]
5. **C-18/Corbett G-92**	69.7	22%	69.7	34%
5. **C-18/Corbett S46**	51.3	16%	--[a]	--[a]
6. **Historic Cypress Creek**	7.0	2%	7.0	3%
7. **Pal-Mar**	57.7	18%	57.7	28%
8. **Grove West**	11.1	3%	11.1	5%
9. **Grove East**	10.6	3%	10.6	5%
10. **Jupiter Farms**	21.9	7%	21.9	11%
11. **Wild and Scenic**	6.9	2%	6.9	3%
Totals	320.3	100%	207.4	100%

[a] This basin does not contribute flows to the Northwest Fork of the Loxahatchee River.

634

635   **Tables 12-7** and **12-8** summarize the monthly mean flow for each of the years from
636   1965–2003 for flows over the Lainhart Dam and total flow into Northwest Fork covered by the
637   four flow monitoring stations (Lainhart Dam station, Cypress Creek station, Hobe Grove station,
638   and Kitching Creek station). For flows over Lainhart Dam (**Table 12-7**), mean monthly flows less
639   than 35 cubic feet per second (cfs) are shaded in red, and flow from 35–65 cfs are shaded in light
640   green. These two flow ranges were selected because 35 cfs is the Minimum Flow and Level
641   (MFL) for the Northwest Fork (SFWMD, 2002a), and 65 cfs is defined as a flow target in the
642   model for the development of the Northern Palm Beach County Comprehensive Water
643   Management Plan (SFWMD, 2002b). The Lainhart Dam data (**Table 12-7**) shows that a low-flow
644   period occurred from 1970–1978. For some years, monthly mean flows were less than 35 cfs
645   even during the wet season (June through November). Another low-flow period occurred from
646   1987–1990. Extended high-flow years occurred from 1991–1999. This pattern is consistent with
647   the total Northwest Fork flow presented in **Table 12-8**; mean monthly flows less than 70 cfs are
648   shaded in red, and flows from 70–130 cfs are shaded in light green. The extended low flow dry
649   season periods in the 1960s, 1970s, and 1980s probably coincide with the period during which the
650   floodplain experienced the most significant saltwater encroachment. The high flow regime
651   instituted in the 1990s has likely helped the floodplain hydrologic condition to recover from the
652   preceding dry years.

Table 12-7. Monthly mean flows (cfs) over Lainhart Dam from 1965–2003.

Years	Jan	Feb	Mar	Apr	May	Jun	Jul	Aug	Sep	Oct	Nov	Dec	Annual Mean
							Month						
1965	39	35	14	2	1	14	29	45	10	136	71	10	34
1966	90	76	34	22	53	211	220	127	88	203	63	37	102
1967	22	40	37	18	5	52	89	114	67	193	79	26	62
1968	14	13	7	2	19	302	173	136	197	274	147	62	112
1969	71	45	116	35	154	120	79	131	135	269	173	86	119
1970	113	104	208	237	97	155	112	64	56	71	29	18	105
1971	16	18	12	3	47	19	38	46	136	79	194	73	57
1972	44	39	21	41	191	204	85	50	33	33	68	28	70
1973	28	36	14	9	13	80	66	124	134	168	41	39	63
1974	150	39	45	14	8	131	151	156	54	134	57	63	84
1975	27	30	20	7	33	104	141	31	85	108	39	15	54
1976	9	20	27	5	106	114	30	67	182	72	72	28	61
1977	60	19	10	2	25	33	11	24	271	42	24	139	55
1978	72	30	32	6	14	145	140	145	88	168	263	190	108
1979	193	79	56	47	61	51	31	19	161	146	113	66	85
1980	47	58	39	20	33	29	86	34	32	80	26	17	42
1981	7	9	3	1	2	6	6	152	176	46	53	9	39
1982	12	26	150	200	166	241	124	93	110	145	302	182	146
1983	143	200	172	108	76	141	77	135	268	342	198	157	168
1984	123	86	127	84	102	124	65	48	179	120	196	150	117
1985	72	43	28	61	21	25	65	40	144	110	53	71	61
1986	125	42	102	82	14	93	112	72	76	80	92	99	83
1987	112	36	69	25	15	24	43	30	39	137	234	34	67
1988	57	47	42	14	29	91	116	184	75	18	14	7	58
1989	4	2	17	8	7	8	30	85	25	79	14	15	25
1990	11	6	7	10	7	15	17	77	93	151	22	16	36
1991	142	118	53	141	119	160	128	86	134	192	92	83	121
1992	49	117	66	56	20	122	125	188	217	164	198	95	118
1993	231	204	200	122	92	104	87	85	164	281	149	89	150
1994	96	142	84	82	70	143	114	223	273	209	278	285	166
1995	140	96	98	85	69	101	131	288	186	352	271	153	165
1996	82	73	156	116	137	140	176	96	128	163	123	78	123
1997	81	104	84	121	93	214	109	200	222	105	83	149	130
1998	148	204	161	88	106	53	84	66	208	133	289	102	136
1999	227	89	70	39	30	172	122	109	198	335	206	109	142
2000	81	74	62	91	34	19	40	18	52	174	29	23	58
2001	16	9	46	24	8	43	197	260	254	236	145	78	110
2002	69	125	60	44	15	116	185	57	40	51	43	36	70
2003	22	14	62	46	119	137	48	149	90	73	146	75	82
Monthly Mean	78	65	67	54	57	104	94	104	130	151	120	77	92

Table 12-8. Monthly mean flows (cfs) into the Northwest Fork of the Loxahatchee River passing the Lainhart Dam, Cypress Creek, Hobe Grove Ditch, and Kitching Creek Flow stations from 1965–2003.

Years	Jan	Feb	Mar	Apr	May	Jun	Jul	Aug	Sep	Oct	Nov	Dec	Annual Mean
						Month							
1965	89	106	56	16	10	44	95	129	34	457	259	53	112
1966	281	258	115	82	184	678	682	418	271	628	206	125	328
1967	83	132	122	68	35	158	270	336	210	607	238	94	197
1968	60	54	39	23	74	952	530	420	652	848	436	181	356
1969	204	136	346	108	438	372	256	395	426	876	523	253	363
1970	337	300	671	728	268	452	328	178	167	200	93	64	315
1971	58	64	48	28	148	68	121	135	403	246	633	239	182
1972	138	133	78	137	593	639	252	155	107	110	222	95	221
1973	99	121	59	44	56	242	205	405	408	517	134	126	202
1974	483	133	145	53	39	367	428	479	175	398	181	181	257
1975	89	95	65	36	107	299	436	107	260	323	124	59	167
1976	40	77	80	29	332	354	100	208	560	227	220	99	193
1977	193	67	44	22	95	97	41	78	853	142	84	406	177
1978	234	102	106	32	50	504	449	438	244	522	840	573	343
1979	544	226	152	139	164	147	91	62	517	483	342	192	255
1980	152	173	122	66	110	95	260	107	120	285	106	70	139
1981	39	53	25	18	16	26	28	476	542	154	188	43	134
1982	55	103	504	685	566	749	417	284	356	458	983	476	470
1983	455	656	552	330	203	418	202	388	853	1,074	606	487	517
1984	367	247	382	237	300	345	166	130	563	360	615	466	348
1985	192	116	83	183	65	89	185	115	448	350	160	210	183
1986	400	122	336	232	51	272	341	259	237	255	305	334	263
1987	335	113	218	84	62	88	134	89	143	441	741	119	214
1988	176	154	138	52	92	250	348	583	254	73	58	36	185
1989	30	24	62	38	30	32	88	233	88	246	58	58	83
1990	49	41	34	42	31	46	63	243	333	435	85	68	123
1991	495	374	161	417	345	481	361	267	400	594	282	240	368
1992	147	326	179	160	64	372	415	584	645	496	632	293	359
1993	740	619	598	340	244	274	233	237	447	867	416	238	437
1994	269	438	225	216	185	465	344	670	842	675	887	874	507
1995	417	275	284	227	172	256	343	858	568	1,146	812	401	482
1996	228	186	430	304	380	389	545	270	383	543	409	225	359
1997	247	300	241	372	262	689	343	594	671	314	224	446	392
1998	431	639	485	233	279	133	228	174	661	414	908	301	404
1999	749	261	181	103	84	495	343	299	599	1,079	606	314	427
2000	216	187	161	255	100	60	114	56	150	516	85	73	165
2001	53	37	126	66	39	149	477	794	792	668	387	203	318
2002	175	343	156	151	51	288	532	164	114	138	115	102	193
2003	65	47	202	136	372	392	126	354	235	184	381	181	224
Monthly Mean	241	201	205	166	172	314	280	312	403	470	374	231	281

653   Because of the hydrologic variability during the past 39 years, the 39-year daily flow data at
654   Lainhart Dam were analyzed to determine the daily flow distribution for each of the 12 months of
655   all the 39 years. This analysis indicates that the daily flow distribution in a month during the
656   39 years is not normally distributed. The results are summarized in **Figure 12-9** which plots the
657   median flow and the 75th percentile flow in the month. The 75th percentile flow represents the
658   flow that is exceeded by only 25 percent of days in that month during the 39 years. Daily flow
659   from Lainhart Dam is less than 50 cfs for 50 percent of time during the months of February,
660   March, April, and May. Flows in April and May are the lowest among all the months. This also
661   shows the importance of flow augmentation during these low flow months.

662

663

664
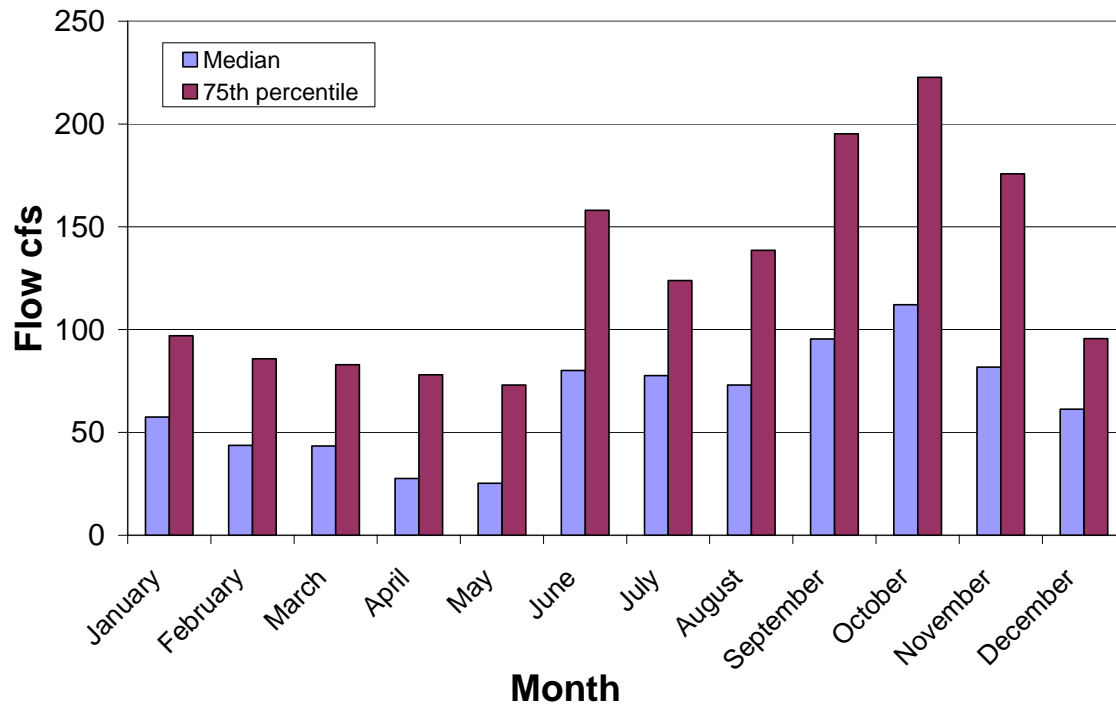
Figure 12-9. Monthly median flow and the 75th percentile flow over
Lainhart Dam from 1965–2003.

665	# MODELING SALINITY

THE HYDRODYNAMIC/SALINITY (RMA) MODEL DESCRIPTION

666

667   Salinity in the Northwest Fork of the Loxahatchee River and Estuary is controlled by both
668   freshwater inflows and tidal circulation, which represent the competition between river and ocean
669   influences. A hydrodynamic/salinity (RMA) model was developed to study the influence of
670   freshwater flows from the tributaries of the Northwest Fork and S-46 on the salinity conditions in
671   the Loxahatchee River and Estuary. In parallel with model development, a data collection
672   network was established to measure tide and salinity at five sites from the embayment area near
673   the Jupiter Inlet (RM 0.70) to RM 9.12. The objective of salinity data collection and model
674   development was to establish the relationship between salinity and the amount of freshwater
675   inflow. The requirement to the model is to predict daily average salinity over a long period of
676   time such as 30 years under various project scenarios. The main focus of the data collection and
677   salinity modeling has been on the upper Northwest Fork of the Loxahatchee River.

678   The software programs used in developing the Loxahatchee River hydrodynamics/salinity
679   model were RMA-2 and RMA-4 (USACE, 1996). RMA-2 is a 2-D depth-averaged finite element
680   hydrodynamic numerical model. It computes water surface elevations and horizontal velocity
681   components for subcritical, free-surface flow in two dimensional flow fields. RMA-2 computes a
682   finite element solution of the Reynolds form of the Navier-Stokes equations for turbulent flows.
683   Friction is calculated with the Manning's n or Chezy equation, and eddy viscosity coefficients are
684   used to define turbulence characteristics. Both steady and unsteady state (dynamic) problems can
685   be analyzed. The program has been used to calculate water levels and flow distribution around
686   islands; flow at bridges having one or more relief openings, in contracting and expanding reaches,
687   into and out of off-channel hydropower plants, at river junctions, and into and out of pumping
688   plant channels; circulation and transport in water bodies with wetlands; and general water levels
689   and flow patterns in rivers, reservoirs, and estuaries.

690   The water quality model, RMA-4, is designed to simulate the depth-average
691   advection-diffusion process in an aquatic environment. The model is used for investigating the
692   physical processes of migration and mixing of a soluble substance in reservoirs, rivers, bays,
693   estuaries, and coastal zones. This model was used to evaluate salinity and the effectiveness of
694   various restoration scenarios. For complex geometries, the model utilizes the depth-averaged
695   hydrodynamics from RMA-2.

696   **IMPLEMENTING THE RMA MODEL**

697   **Model Setup**

698   Based on the most recent bathymetry, freshwater inflow and tide data, the RMA model was
699   updated in early 2004. The current model mesh includes a total of 4,956 nodes with elevations
700   derived from the survey data provided by USGS. **Figure 12-10** shows the RMA model mesh
701   construction with 1,075 quadrilateral elements and 231 triangular elements. Arrows in the figure
702   indicate the locations where freshwater inflows are applied. The four tributaries that contribute
703   freshwater to the Northwest Fork are Lainhart Dam, Cypress Creek, Hobe Grove Ditch, and
704   Kitching Creek. The RMA model domain also includes the Southwest Fork and flows from the
705   S-46 structure. The RMA itself does not predict the amount of freshwater entering the system
706   from the watershed or discharge structures. The freshwater discharge amounts from these
707   tributaries and structures are provided by the WaSh model or from recorded data from the flow
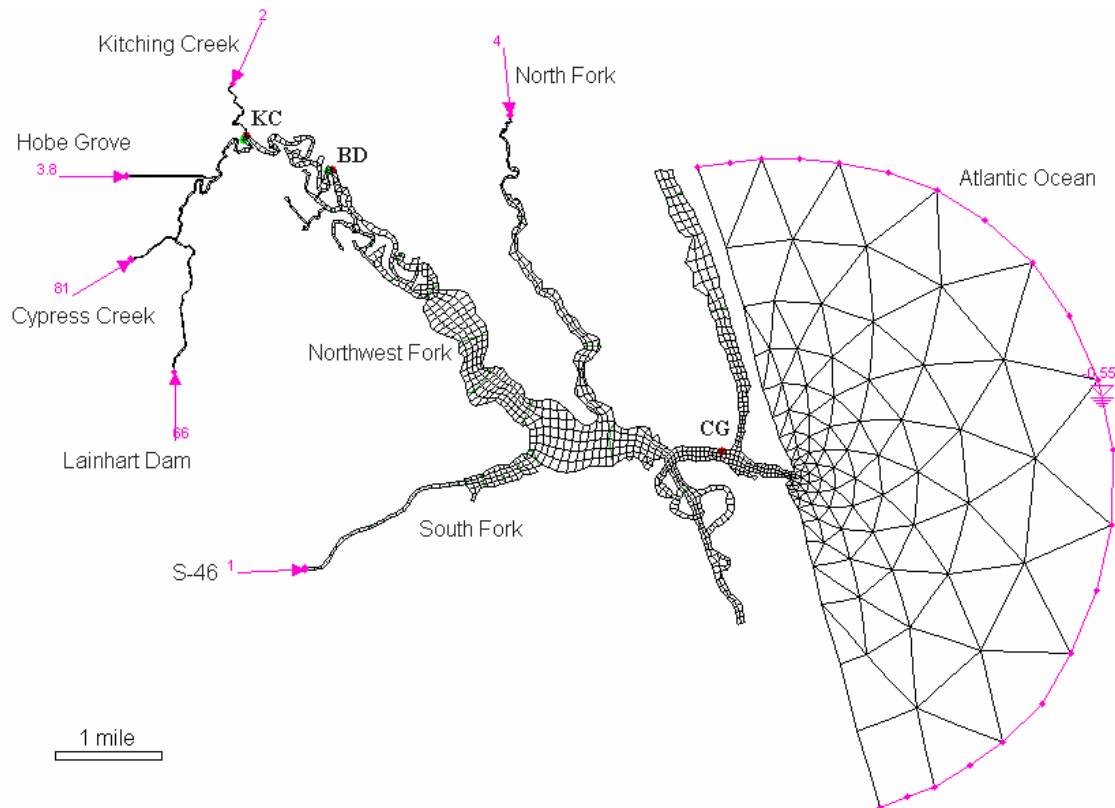708   gauges.

Figure 12-10. The RMA model domain map. KC = Kitching Creek USGS
Station; BD = Boy Scout Dock Station, CG – US Coast Guard Station.

709   The meandering river channel pattern is one of the fundamental characteristics of the natural
710 system of the Northwest Fork of the Loxahatchee River. The previous studies have demonstrated
711 that restoring the natural oxbows to the Northwest Fork can effectively reduce saltwater intrusion
712 into the historically freshwater reaches. The meandering river channel and oxbows of the
713 Northwest Fork are preserved in the construction of the RMA model mesh.

714   Several natural river channel restoration projects have been implemented in the past decade to
715 restore oxbows to the Northwest Fork. Salinity measurements taken before and after the
716 implementation of the projects indicate that the oxbows can reduce the extent of saltwater
717 intrusion to the Northwest Fork. The RMA model mesh contains the geographic features of the
718 river channel. Depending on the time period, the model simulation can be conducted with the
719 oxbow restoration projects completed for the post-project period or without the restored oxbows
720 for the pre-project period. The current model mesh is also detailed enough to simulate the
721 effectiveness of potential channel restoration projects in river reaches up to the Trapper Nelson
722 Interpretive Site. The channel above the Trapper Nelson Interpretive Site will be further refined
723 in the mesh after an ongoing GIS project is completed that will provide more detailed geometry
724 for the river channel above the Trapper Nelson Interpretive Site. On the ocean side, the model
725 mesh was extended three miles offshore into the Atlantic Ocean to obtain a relatively stable
726 salinity boundary condition (Hu, 2004).

727   The RMA model was applied to establish the relationship between the amount of freshwater
728 inflow and the salinity regime in the Northwest Fork. The freshwater/salinity relationship
729 provided means to assess restoration plan scenarios.

Model Verification

731   In parallel with the preliminary RMA model setup, a data collection program was
732 implemented. A bathymetric survey was conducted by the U.S. Geological Survey (USGS) in
733 early 2003. Water depth was recorded along survey lines in the Northwest Fork and the North
734 Fork of the Loxahatchee River. The Northwest Fork survey covered river reaches from RM 4.0 to
735 the Trapper Nelson's Interpretive Site (RM 10.50). Approximately three miles of the North Fork
736 were also surveyed. In addition to the flow gauges located at Lainhart Dam and Kitching Creek,
737 two additional gauges were established on Cypress Creek and Hobe Grove Ditch in November
738 2002. These four flow gauges monitor the majority of freshwater input to the Northwest Fork.
739 Four tide and salinity stations have also been deployed in the estuary since November 2002 by the
740 USGS. An additional tide/salinity gauge was installed at RM 9.12 in October 2003 by the
741 District's Water Supply Department. These five tide/salinity stations monitor the tide and salinity
742 in the estuary continuously and record the data at 15-minute intervals. The data is retrieved at
743 scheduled maintenance times and reported quarterly after quality assurance and quality control
744 (QA/QC) has been conducted. To detect temperature and salinity stratification, three of the
745 tide/salinity stations record salinity and temperature measurements at two water depths. The three
746 sites with double temperature/salinity sensors are located at RM 9.12, Boy Scout Camp dock
747 (RM 5.92) and the U.S. Coastal Guard Station near the Jupiter Inlet (RM 0.70). All sensors were
748 installed at water levels below lower low tides to avoid exposure to air.

749   In addition to tide and salinity measurements obtained from the USGS sites, the Loxahatchee
750 River District (LRD) also has an estuarine data collection program at several additional locations
751 that are not covered by the USGS monitoring network. The LRD uses multi-parameter datasondes
752 to record time, dissolved oxygen, water depth, conductivity/salinity, pH, and temperature. The
753 meters are located near the bottom of the channel in order to track maximum salinity changes in
754 the water column. The LRD data were collected at North Bay seagrass survey site (RM 1.48),
755 Pennock Point seagrass survey site (RM 2.44), Northwest Fork near the mouth of Kitching Creek
756 (RM 8.13), Station 66 in the Wild and Scenic Loxahatchee River, and Station 69 near the

757 Indiantown Road (RM 14.93). To measure current velocity, the LRD contracted Scientific
758 Environmental Applications to install two bottom mount Acoustic Doppler Current Profiler
759 (ADCP) units at various locations in the estuary in 2003.

760   The Loxahatchee hydrodynamic/salinity (RMA) model was verified against field data for the
761 period from May 1 to August 12, 2003. **Figure 12-11** shows the combined freshwater inflow
762 from four major tributaries to the Northwest Fork for this period. Daily averaged flow rates (cfs)
763 from flow gauges on upper Northwest Fork at Lainhart Dam, Cypress Creek, Hobe Grove, and
764 Kitching Creek were used for the calculation. Discharge from S-46 into the South Fork was based
765 on measurements at the discharge structure for the model simulation period.

766   **Figure 12-12** is a comparison of tidal data from the Coast Guard station (RM 0.70) with the
767 RMA-2 model output for the same location. Because the two curves overlap each other when
768 printed in the same chart, the model output and field data are plotted in separate charts using the
769 same scale and grid lines for ease of comparison. For RMA-4 applications, a constant salinity of
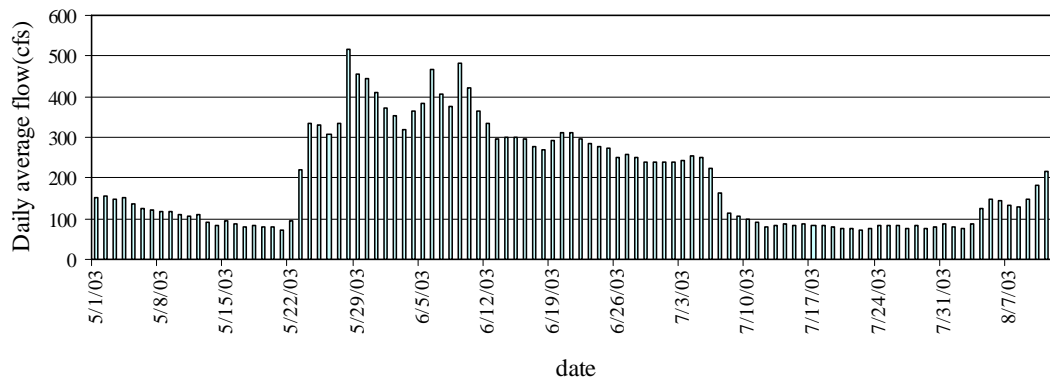770 35.5 ppt was applied on the ocean boundary.

Figure 12-11. Freshwater inflow from major tributaries to the Northwest
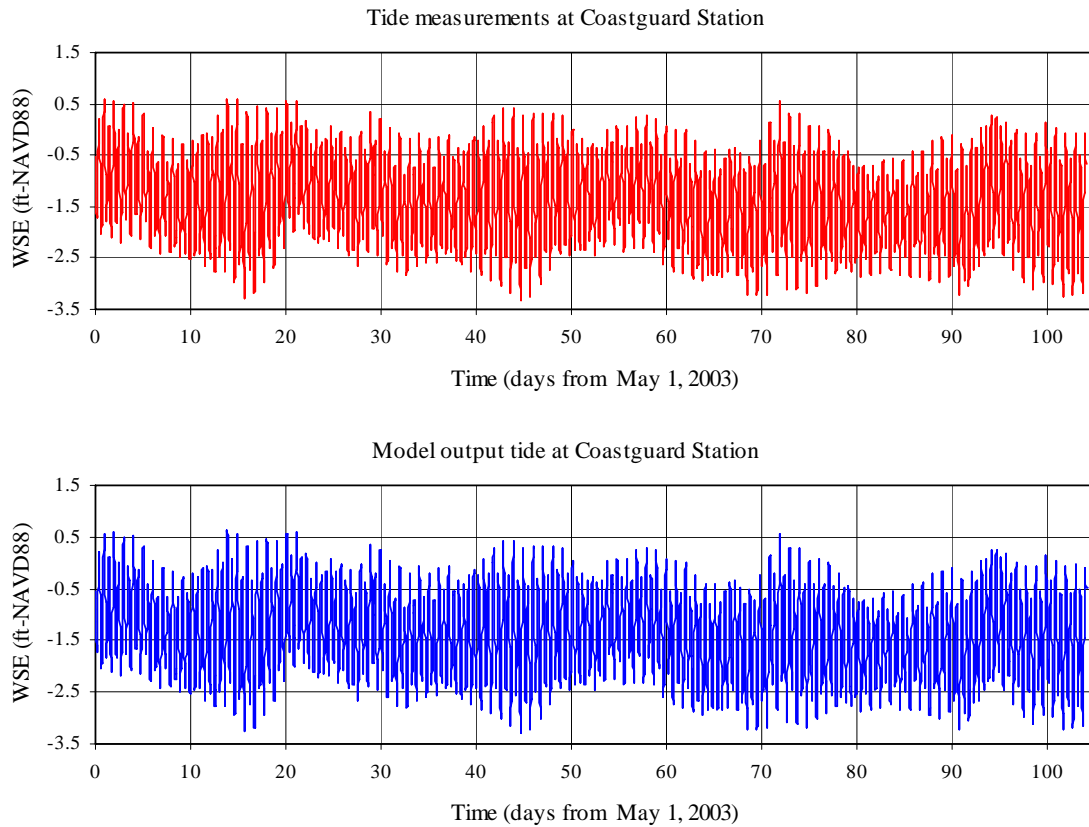Fork of the Loxahatchee River.

Figure 12-12. Tide measurements at the Coast Guard Station (RM 0.70): field data and RMA model output.

771   Field data and model output of tides at Boy Scout Dock (RM 5.92) and Kitching Creek
772   (RM 8.13) are plotted in **Figure 12-13** for comparison. The two stations are approximately 2 river
773   miles apart and there is no major tributary between these locations. Both field data and model
774   output indicate that the tidal regimens at these two sites are similar in terms of range.

775   **Figure 12-14** compares model output of depth-averaged salinity with actual field salinity
776   measurements from instruments at fixed elevations However, although these two quantities are
777   similar, they do not represent the same physical parameters and are not directly comparable. The
778   difference between the model output (representing depth-averaged salinity) and the actual field
779   measurement (representing salinity at a fixed depth) could be significant when the system is
780   stratified.

781   The salinity record at Boy Scout Dock increased to 10 parts per thousand (ppt) between
782   Day 50 and Day 60. This sudden salinity increase does not seem to be related to or supported by
783   data from other field records. A salinity of 10 ppt usually occurs at this site when freshwater
784   inflow is below 100 cfs. The flow gauges actually recorded over 200 cfs for this period. The
785   salinity record from the adjacent Kitching Creek station is also inconsistent with the salinity
786   increase at the Boy Scout Dock station. Previous studies indicated that 10 ppt at Boy Scout Dock
787   station would have raised salinity at Kitching Creek station to 2 ppt or above (Russell &
788   McPherson, 1984); however, there was no salinity increase for Kitching Creek during this time
789   period (see the Kitching Creek chart in **Figure 12-14**). Therefore the accuracy of the salinity field
790   measurements at Boy Scout Dock between Day 50 and Day 60 is questionable.

791   Both RMA-2 and RMA-4 are two-dimensional depth-averaged models. When the system is
792   minimally stratified, such as the condition near the Jupiter Inlet at the Coast Guard station, the
793   modeled salinity output tracks the field salinity data rather closely. However, when the system is
794   highly stratified, as occurs in certain areas, the modeled salinity output for that area could give a
795   smaller salinity variation between high tide and low tide when compared to the field salinity
796   measurements from fixed depths (see the Boy Scout Dock chart in **Figure 12-14**).

797   The RMA-4 output is depth-averaged salinity, which differs from salinity measured by a
798   transducer at a fixed elevation. The conductivity transducers were installed at elevations that
799   would remain below the water surface at low tide. Because the range between higher high and
800   lower low water is close to 4 feet and the overall water depth is only about 6 feet to 10 feet, the
801   conductivity transducers would be situated in the lower water column during high tide. Under
802   these conditions, the instrument would take measurements from the surface layer at low tide and
803   from the bottom layer at high tide. If the system is well mixed (i.e., no stratification), then there
804   should be no difference between the modeled depth-averaged salinity and field salinity
805   measurements. However, when the system is stratified, the daily salinity variation recorded by the
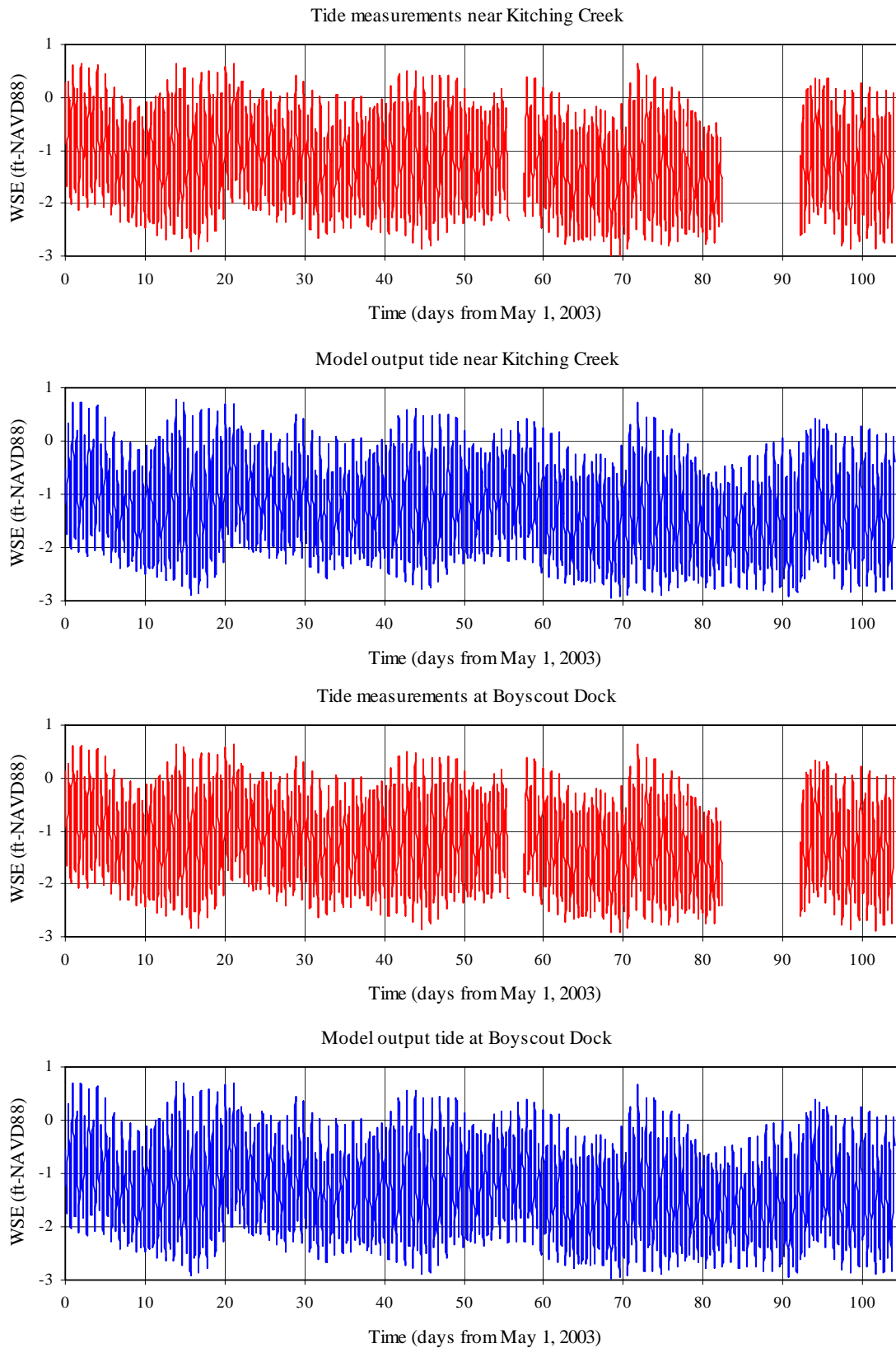806   instruments would be wider than the daily salinity variation output from depth-averaged salinity
807   model.

Figure 12-13. Tide at Boy Scout Dock (RM 5.92) and Kitching Creek
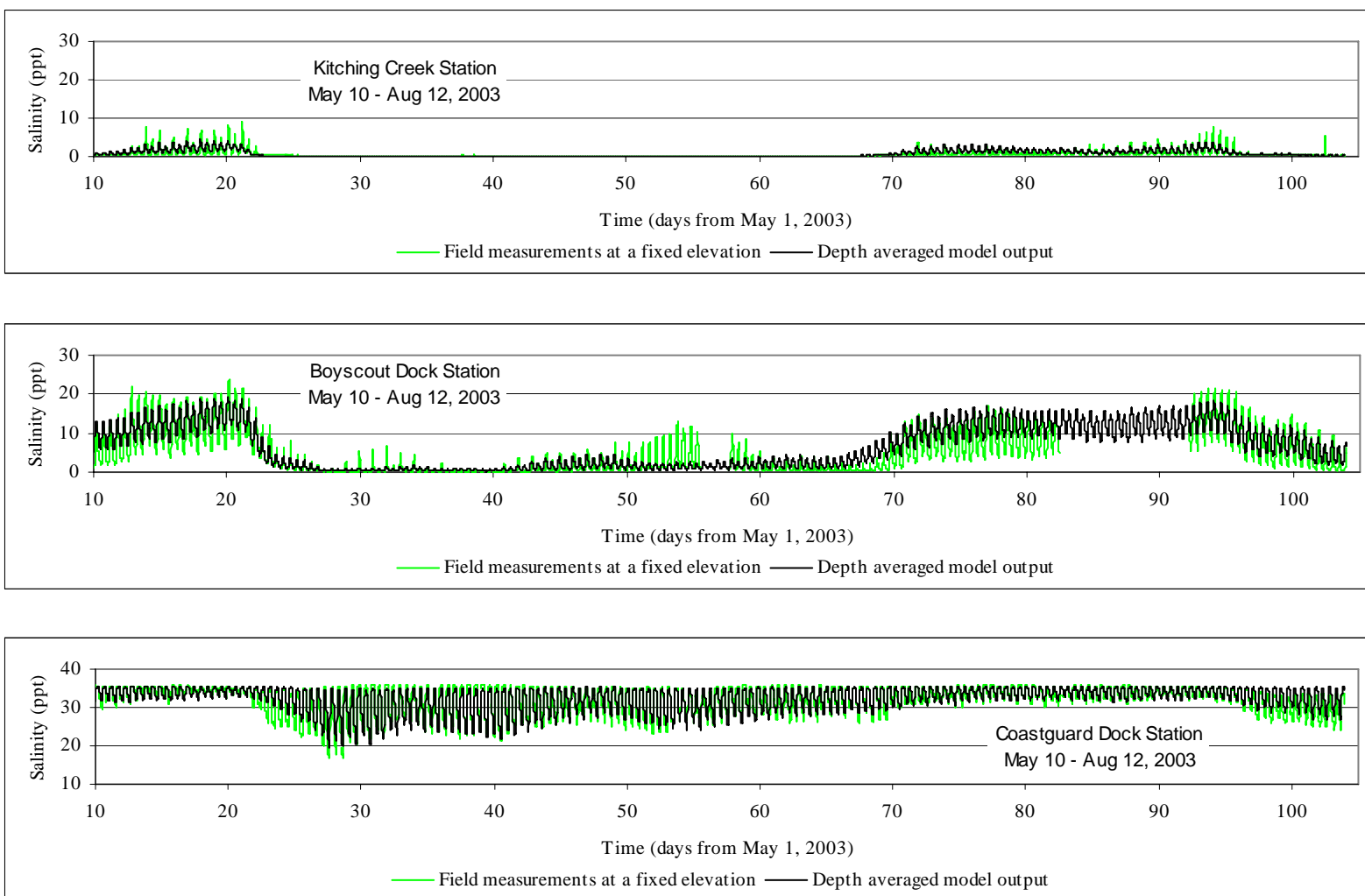(RM 8.13) stations – field data and model output.

Figure 12-14. Model output of depth-averaged salinity and field measurements at fixed elevations in the water column.

808   The most likely reason for the difference between model prediction and field measurements is
809   that there is additional freshwater inflow to the system that bypasses the four stations on the river
810   and the major tributaries. Such additional sources of freshwater may include overland flow and
811   groundwater seepage into the system. A groundwater monitoring network that was established in
812   2003 indicates active exchanges between the river and the groundwater table. The model
813   predicted higher salinity at the beginning of dry periods when the groundwater tables are still
814   relatively high and therefore provide additional freshwater to the system. Including groundwater
815   input in the model will likely increase the accuracy in salinity prediction. The current model,
816   without the input of groundwater input and overland flow, tends to be conservative (predicting
817   higher salinity).

818   The current model does not include driving forces such as wind, precipitation/evaporation
819   and the exchange between the river and the groundwater which can be significant in the upper
820   river reaches. The model verification simulation, which was only driven by major tributary
821   freshwater input and ocean tide, was able to predict the tide regimen rather accurately and predict
822   the trend of salinity changes over the 3-month simulation period that included both low and high
823   freshwater input to the estuary. This seems to indicate that the amount of freshwater inflow to the
824   estuary and tide are the two most dominant factors that affect the salinity regimen in the upper
825   Northwest Fork.

826 ## RMA MODEL SIMULATION RESULTS – FRESHWATER INFLOW
827 ## AND SALINITY RELATIONSHIP

828   The tidal circulation and salinity structure of estuaries involves competition between
829   freshwater river flows and ocean influences. River flow persistently adds freshwater to the
830   estuary, however saltwater may still penetrate far inland due to gravitational and diffusive fluxes
831   (MacCready, 2004). Although there are other factors in addition to tide and freshwater inflows
832   that affect the salinity regime, the analysis of the field data from the Loxahatchee River suggested
833   that tide and freshwater inflow are the two most important factors that determine the salinity
834   conditions in the Northwest Fork (Hu, 2004). To establish the relationship between freshwater
835   inflow and salinity in the Northwest Fork of the Loxahatchee River, the RMA model was used in
836   12 modeling scenarios where the amount of total freshwater flow from all three forks of the
837   Loxahatchee River into the estuary was held constant for rates varying from 40 cfs at the low
838   flow end to 7,000 cfs at the high flow end. These flow rates were determined based on an analysis
839   of freshwater inflows simulated by the watershed model (WaSh). During RMA model output
840   processing, 15 study sites were identified for ecological assessment where salinity predictions are
841   needed. Information about study and assessment sites is provided in **Table 12-9**. Sites noted as
842   USGS stations are locations where tide and salinity measurement data are collected by U.S.
843   Geological Survey as discussed in the previous sections. **Figure 12-15** shows the locations of the
844   15 assessment sites.

845

846

Table 12-9. Salinity and ecological assessment sites.

847

Coordinates[a]		Site		Description
X (feet)	Y (feet)	Station ID	River Mile	
955325	951200	CG	0.70	USGS Coast Guard
951456	952232	SGNB	1.48	Seagrass site - North Bay
949616	951344	SGSB	1.74	Seagrass site - Sand Bar
949538	950648	PD	1.77	USGS Pompano Drive
945680	951761	SGPP	2.44	Seagrass site - Pennock Point
945105	953335	O1	2.70	Oyster site 1
942902	954999	O2	3.26	Oyster site 2
942332	957383	O3	3.74	Oyster site 3
940923	958927	O4	4.13	Oyster site 4
938854	961625	O5	4.93	Oyster site 5
936681	963169	O6	5.45	Oyster site 6
935708	965258	BD	5.92	USGS Boy Scout Dock
934679	966363	VT9	7.06	Vegetation Transect 9
931399	966948	KC	8.13	USGS Kitching Creek
929733	964696	RM9	9.12	USGS RM 9.1; Vegetation Transect 7

[a] State Plane Florida East NAD83.
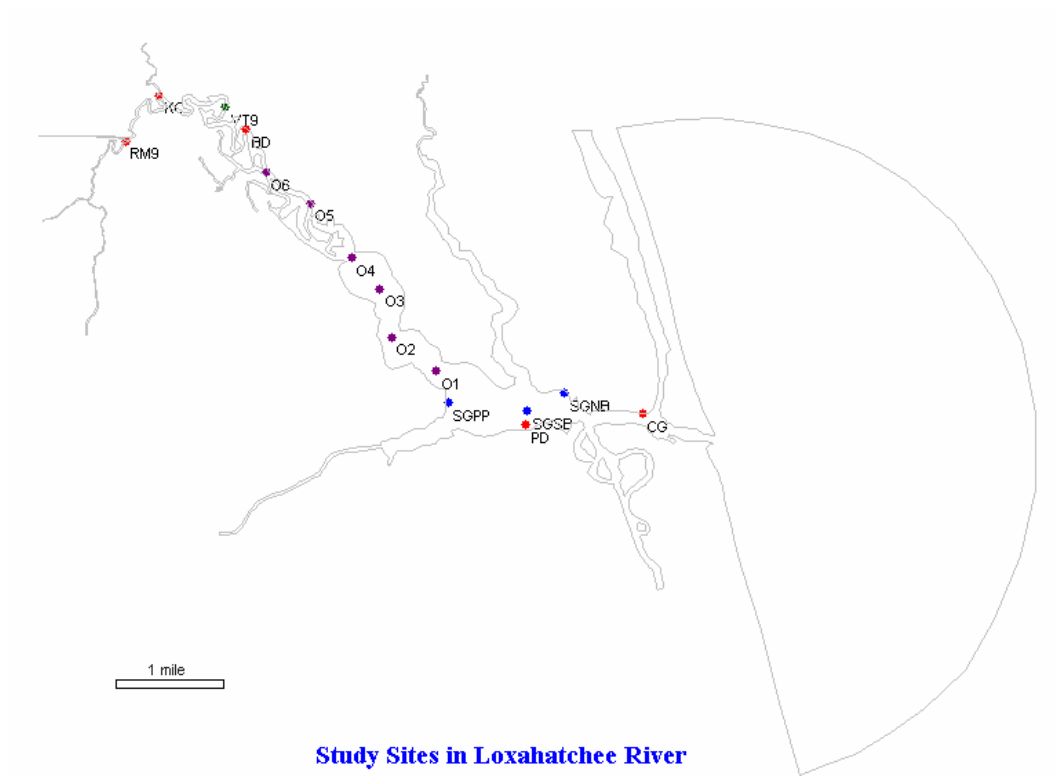
Study Sites in Loxahatchee River

Figure 12-15. Location of salinity and ecological assessment sites. Red dots represent USGS sites; blue dots represent seagrass sites; purple dots represent oyster sites; and green dots represent vegetation sites.

848   The objective of the RMA model application is to establish a relationship between the amount
849 of freshwater inflow and tidally averaged salinity. The RMA model output was averaged over a
850 lunar month that includes a full lunar tidal cycle with both spring and neap tides. Thus, these
851 results reflect the daily averaged salinity under an average tidal condition.

852   **Table 12-10** is a summary of the RMA model output of average salinity for 12 flow scenarios
853 at each of the 15 sites. Regression analysis of the results yielded regression equations with
854 excellent curve fitting. The best fit ($R^2 = 0.999$ for all the 15 sites) was achieved with exponential
855 functions in the form of

856

857 $$Y = Y_0 + a\ e^{-bX}$$ [11]

858

859 where X is freshwater inflow in cubic feet per second and Y is salinity in parts per thousand. Y_0,
860 a, and b are regression parameters that are listed in **Table 12-10** for each of the 15 sites.

Table 12-10. Tidally averaged salinity (ppt) versus freshwater inflow (cfs) for the 15 study sites in the Loxahatchee River.

Flow(cfs)	CG	SGNB	SGSB	PD	SGPP	O1	O2	O3	O4	O5	O6	BD	VT9	KC	RM9
40	34.6	34.1	33.9	33.8	33.2	32.7	32.0	31.1	30.5	27.8	25.8	23.6	16.8	9.7	4.2
70	34.4	33.6	33.3	33.2	32.3	31.7	30.5	29.2	28.3	24.4	21.6	18.8	11.0	4.9	1.4
100	34.1	33.1	32.7	32.7	31.5	30.6	29.0	27.4	26.2	21.5	18.1	15.0	7.2	2.5	0.5
150	33.7	32.4	31.8	31.7	30.1	29.0	26.8	24.7	23.1	17.3	13.5	10.3	3.6	0.9	0.2
200	33.3	31.6	30.9	30.8	28.8	27.4	24.8	22.2	20.4	13.9	10.0	7.1	1.9	0.4	0.2
300	32.5	30.1	29.1	29.0	26.4	24.5	21.1	18.0	15.9	9.1	5.6	3.4	0.6	0.2	0.2
500	31.0	27.4	26.0	25.8	22.2	19.6	15.4	11.8	9.6	3.9	1.8	0.9	0.2	0.2	0.2
800	28.8	23.8	21.8	21.6	17.1	14.0	9.6	6.3	4.6	1.2	0.5	0.3	0.2	0.2	0.2
1200	26.1	19.6	17.3	17.0	12.1	9.0	5.2	2.8	1.8	0.4	0.2	0.2	0.2	0.2	0.2
2400	19.3	10.9	8.5	8.3	4.3	2.5	0.9	0.4	0.3	0.2	0.2	0.2	0.2	0.2	0.2
4800	10.1	3.1	1.9	1.8	0.6	0.4	0.2	0.2	0.2	0.2	0.2	0.2	0.2	0.2	0.2
7000	5.0	0.6	0.3	0.3	0.2	0.2	0.2	0.2	0.2	0.2	0.2	0.2	0.2	0.2	0.2
y0	-3.074	-0.753	-0.334	-0.291	0.118	0.223	0.225	0.215	0.219	0.224	0.2	0.19	0.16	0.153	0.151
a	38.04	35.51	34.99	34.94	34.25	34.02	33.83	33.68	33.52	32.92	32.47	31.83	29.3	24.76	19.4
b	3E-04	6E-04	7E-04	7E-04	0.001	0.001	0.002	0.003	0.003	0.006	0.008	0.01	0.018	0.03	0.049

861   The freshwater flow versus salinity relationships tabulated in **Table 12-10** are plotted in
862   **Figures 12-16** and **12-17**. Each curve in **Figure 12-16** represents the flow/salinity relationship for
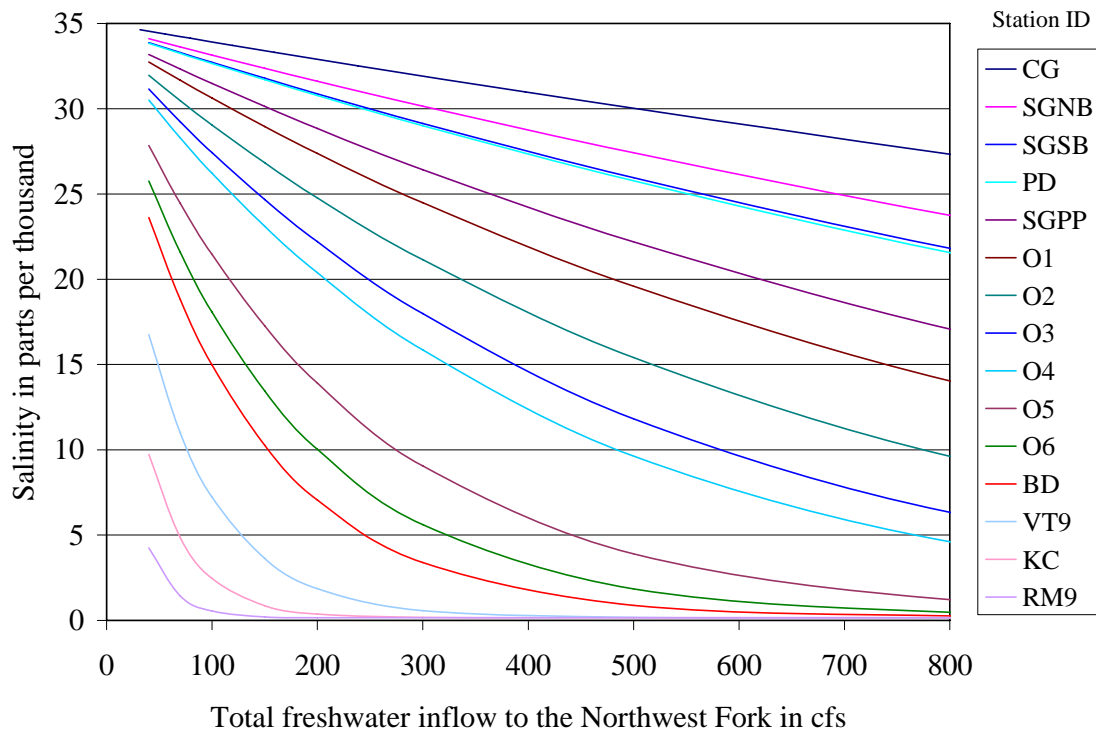863   each of the 15 sites. For each site, salinity increases as freshwater inflow decreases.

Figure 12-16. The relationship between freshwater inflow and salinity at
the 15 study sites.

864   In order to show the details of salinity variation at low flow end, the charts were plotted only
865   for inflows up to 800 cfs. For salinity regimens with freshwater inflows greater than 1,200 cfs,
866   either **Table 12-10** or Equation [11] can be used to determine the salinity value. The curves in
867   **Figure 12-17** represent the salinity gradients at various levels of freshwater inflow. Each line
868   represents the spatial salinity distribution for a particular inflow scenario.
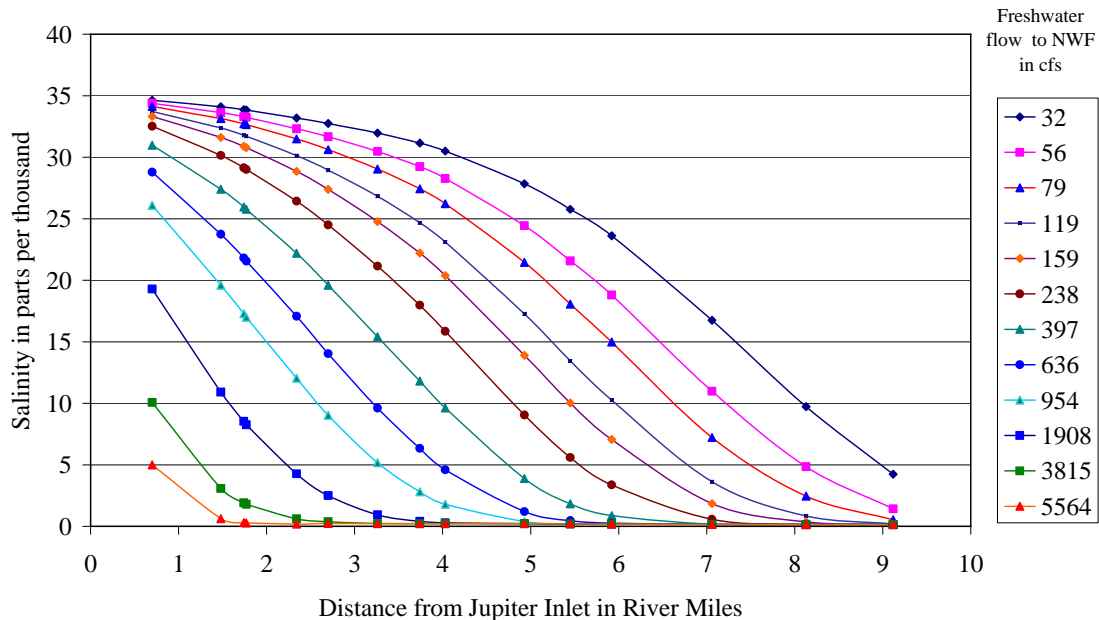
869

870
871

872   **Figure 12-17.** Salinity gradients for various freshwater inflow conditions.

873

874   Although Equation [11] expresses salinity as a single dependent variable function, there are
875   other driving forces that affect salinity including tide, wind, flux between river and groundwater,
876   precipitation, and evaporation. However, the analysis of field data indicated that freshwater
877   inflow is the most important factor affecting salinity. When salinity is plotted against freshwater
878   flow, the data points form a clear trend line. Comparing results from Equation [11] with actual
879   field data provides a reality check. **Figures 12-18** through **12-21** compare the model results from
880   Equation [11] with actual field measurements. As expected, deviations from the modeled
881   flow/salinity curve indicate the existence of other driving forces that affect salinity. Nonetheless,
882   the correlation between salinity and freshwater inflow is significant. Another factor that could
883   cause deviations is that the system is under constant transition in response to the changes in the
884   driving forces. Therefore it is rare for the system to reach equilibrium as the case in the constant
885   flow simulations. The overall trend of the field measurements shows a strong correlation between
886   the amount of freshwater inflow and salinity throughout the estuary.
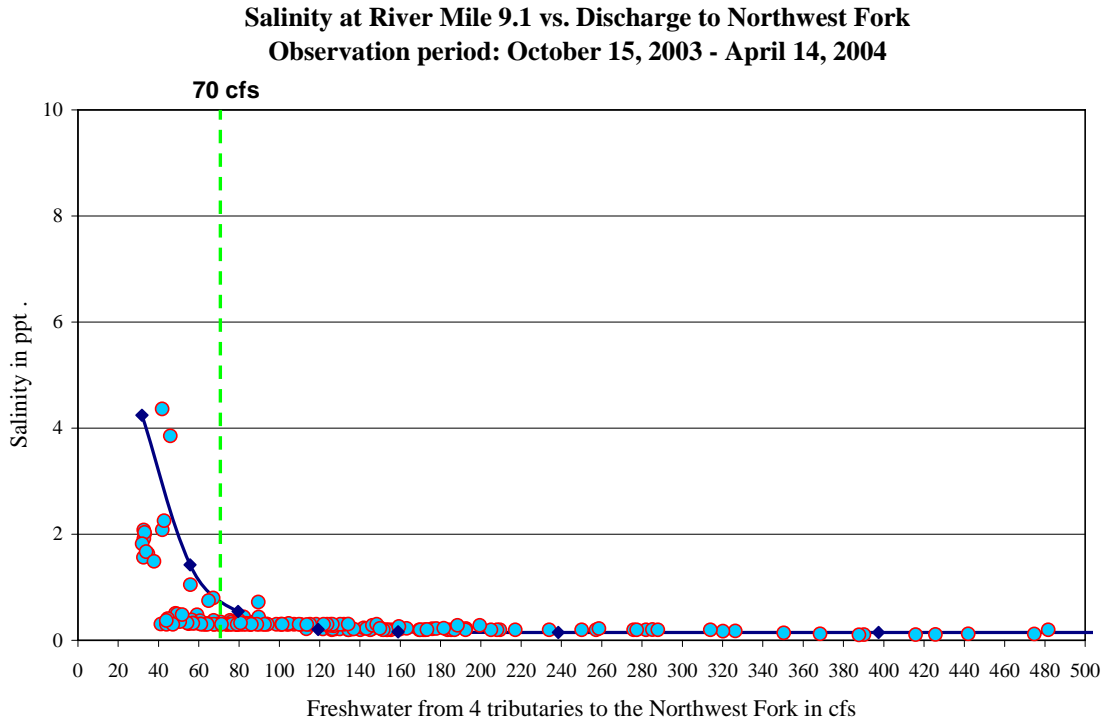
Salinity at River Mile 9.1 vs. Discharge to Northwest Fork
Observation period: October 15, 2003 - April 14, 2004

Figure 12-18. The effects of freshwater inflow on salinity at RM 9.1
from October 15, 2003–April 14, 2004.

Salinity at Kitching Creek Confluence vs. Discharge to Northwest Fork
Observation period: December 11, 2002 - April 14, 2004
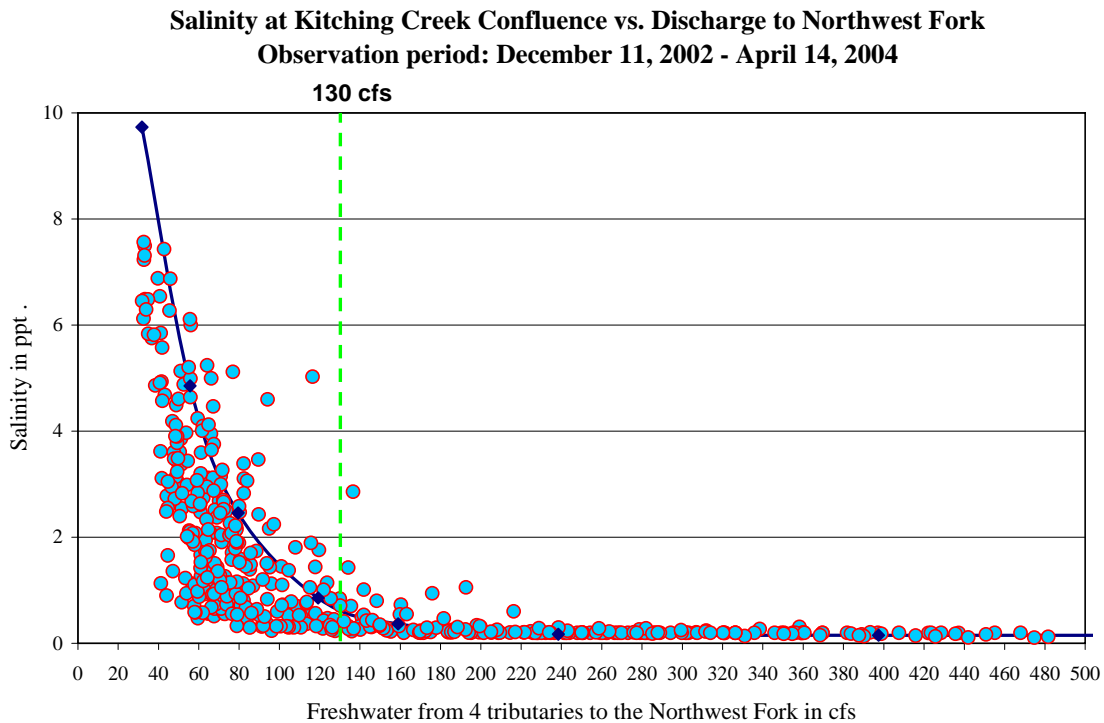
Figure 12-19. The effects of freshwater inflow on salinity at RM 9.1
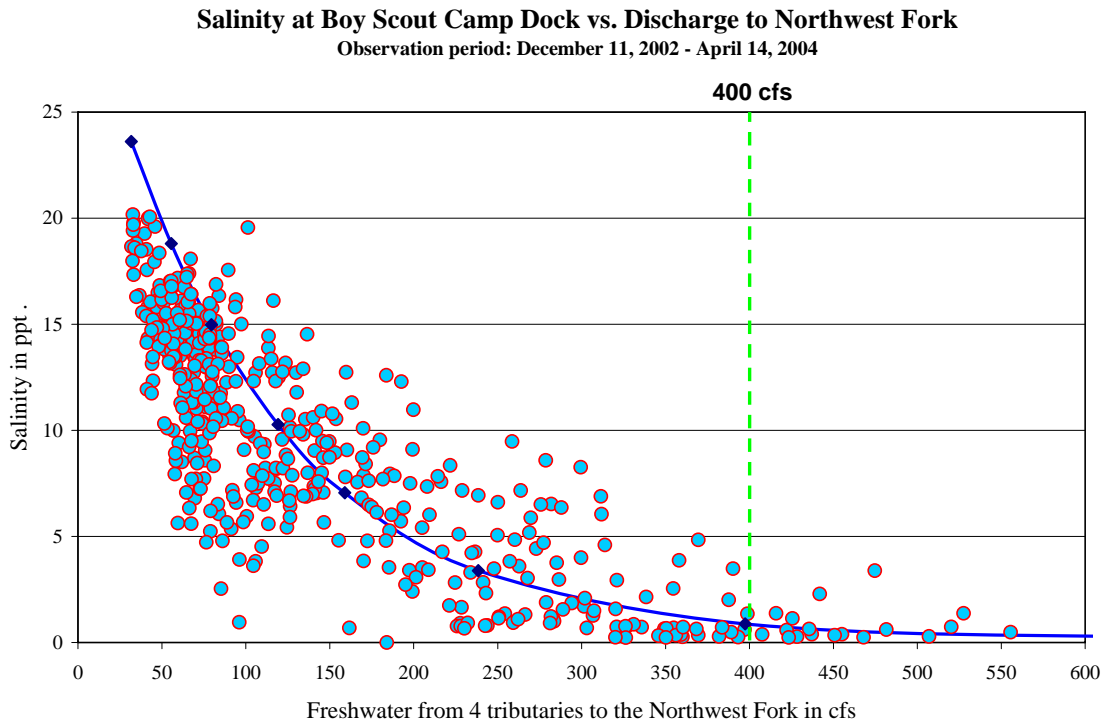from October 15, 2003–April 14, 2004.

Salinity at Boy Scout Camp Dock vs. Discharge to Northwest Fork
Observation period: December 11, 2002 - April 14, 2004

Figure 12-20. The effects of freshwater inflow on salinity at Boy Scout Dock from December 11, 2002–April 14, 2004.

Salinity at Pampano Drive near Sand Bar seagrass site vs. discharge from all major tributaries and canals
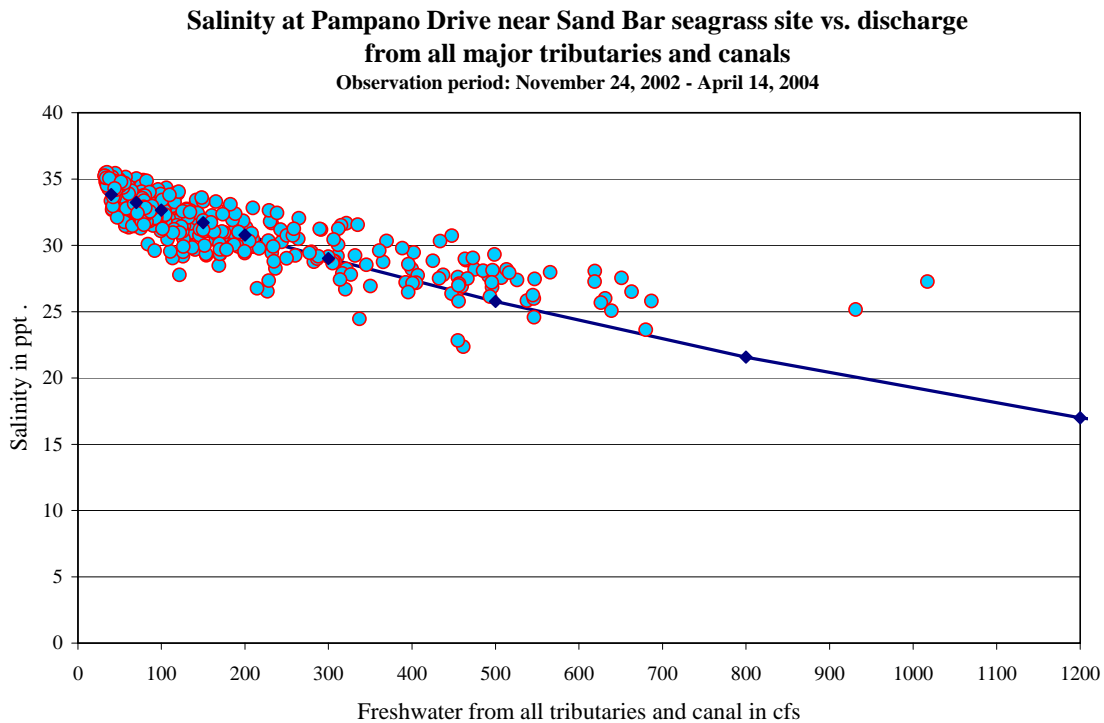Observation period: November 24, 2002 - April 14, 2004

Figure 12-21. The effects of freshwater inflow on salinity at Embayment from November 24, 2002–April 14, 2004.

887   Freshwater inflows to the Northwest Fork from the four major tributaries, several small
888 tributaries and overland flow were modeled. If the inflows from all the tributaries were
889 considered individually, they would form a large array of scenarios. The analysis of the field data
890 indicates that there is a good correlation between salinity at various sites with the total freshwater
891 flow volume to the Northwest Fork. The physical explanation for this correlation is the strong
892 tidal mixing in the Northwest Fork. For example, when the tide rises, freshwater inflows from
893 Kitching Creek will be pushed upstream into the river reaches above the mouth of Kitching Creek
894 and thus influence the salinity there. It is the total volume of freshwater entering the Northwest
895 Fork that matters the most for the reaches between RM 6 and RM 9. The origin of freshwater
896 (whether the freshwater was from Kitching Creek or some other tributary) does not seem to be an
897 important factor in the current analysis. Such a finding has two implications:

898

899 1. Freshwater from all the tributaries affects the salinity in the Northwest Fork. Therefore, any
900   increase of freshwater discharge from any combination of tributaries will help achieve the
901   salinity management goal of the Northwest Fork between RM 6 and RM 9. In addition to
902   increasing freshwater flows from the G-92, flows from other tributaries and basins such as
903   Cypress Creek/Pal Mar, and Kitching Creek should also be fully utilized.

904

905 2. Salinity predictions in the Northwest Fork between RM 6 and RM 9 can be based on total
906   freshwater inflow to the Northwest Fork instead of freshwater inflow from each individual
907   tributary. Such an approach will allow the testing of more restoration scenarios with limited
908   resources. This capability is especially critical in the initial alternative assessment phase of
909   the restoration plan, since numerous scenarios need to be analyzed. When the total amount of
910   freshwater demand is determined, the analysis can then evolve into the next phase that is to
911   consider the freshwater contribution from each tributary individually to meet the Northwest
912   Fork freshwater demand. At that phase, a model with more refined spatial resolution such as
913   the RMA model that was described in the previous sections can be used for scenarios where
914   tributaries are simulated separately from each other.

915

916   The salinity value predicted by Equation [11] is tidally averaged salinity over a lunar tidal
917 cycle. The actual salinity in the river constantly varies in response to tides. If the hourly salinity
918 variation over each tidal cycle needs to be considered, then the information is available from the
919 original model output.

920   **Figure 12-22** is the model output of salinity at the Pennock Point seagrass transect in a lunar
921 month. The graphs are the output under three freshwater inflow conditions. Total freshwater
922 inflows of the three simulations are 500 cfs, 800 cfs, and 1,200 cfs. The amount of freshwater
923 inflow affects both the overall salinity level and the range of salinity variation (the difference of
924 salinity between high tide and low tide).

925   **Figure 12-22** represents the salinity predictions for only one site under three flow conditions.
926 The model simulation output included salinity for 15 sites under 12 different inflow conditions;
927 thus 180 sets of time-series data were produced.

928
929
930
931
932
933
934
935
936
937
938
939
940
941
942
943
944
945
946
947
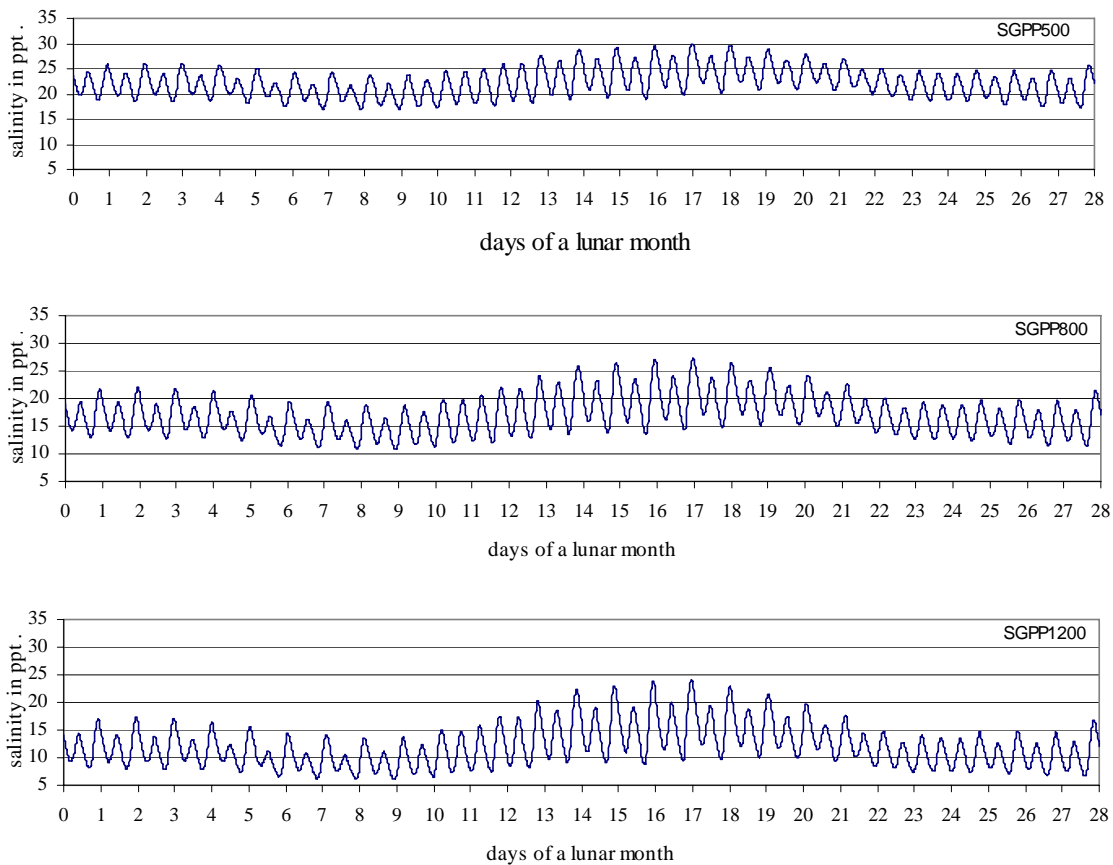948
949
950
951
952
953
954
955

Figure 12-22. Salinity at Pennock Point seagrass transect in a lunar month; total freshwater inflow to the Loxahatchee River: 500, 800, and 1,200 cfs.

956   **Figure 12-22** represents one example from a large array of charts in the model output that
957   cover a wide range of freshwater flow. The salinity conditions represented by 500, 800, and
958   1,200 cfs are relatively high flows that begin to affect salinity conditions at the Pennock Point
959   seagrass site (RM 2.44).

960   The RMA was applied to scenarios with varying amounts of freshwater inflow. Both the field
961   data and model simulation indicated that there is a strong correlation between freshwater inflow
962   and the salinity regimen in the estuary. Based on model output and field data analysis, a
963   relationship was established to predict salinity at various points in the estuary with respect to
964   freshwater inflow rates and tidal fluctuations. The salinity/freshwater relationship was applied in
965   the Loxahatchee River MFL study (SFWMD, 2002a). The RMA model was also used to provide
966   a preliminary assessment of the impacts that inlet deepening and sea level rise have had on the
967   salinity regime in the estuary (Hu, 2002).

968   # LONG-TERM SALINITY MANAGEMENT MODEL

969   The freshwater/salinity relationship described in the previous section was coded into the
970   Loxahatchee Estuary Long-Term Salinity Management Model (LSMM) to predict tidally
971   averaged salinity in response to various restoration scenarios. This model can also simulate
972   system operation rules and calculate the amount of freshwater demand for salinity management.

973   The salinity values in **Table 12-10** are based on an equilibrium state with constant freshwater
974   inflows. In the applications of the freshwater input versus salinity relationships, the dynamic
975   nature of the system needs to be considered. Under natural conditions, freshwater inflow is rarely
976   constant. The salinity conditions observed in the estuary are the result of a series of transitions
977   from one state to the next. The changes in salinity lag behind the changes in freshwater inflow.
978   Following an increase of freshwater inflow, salinity in the estuary will decrease accordingly and
979   gradually approach a new equilibrium state. As the amount of freshwater decreases, the salinity in
980   the estuary will increase gradually. Depending on the direction of salinity changes, the process
981   can be described as an exponential increase or decay. **Figure 12-23** is a graphic description of
982   salinity transition when an increase of freshwater inflow occurs. The dotted line indicates the
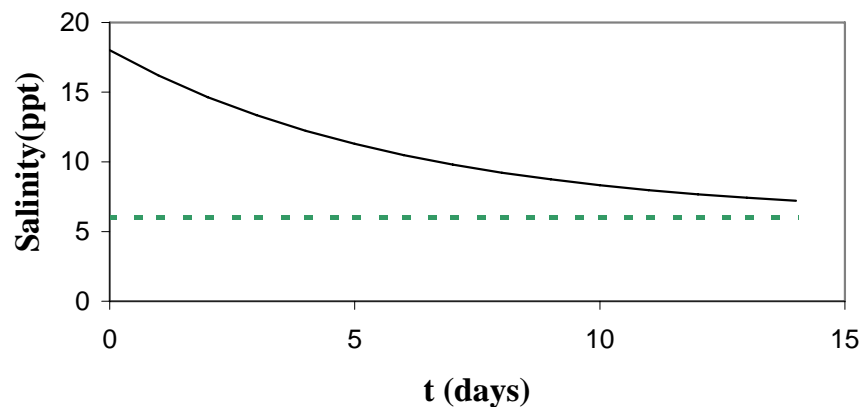983   equilibrium salinity at the higher level of freshwater inflow.
984

985   **Figure 12-23**. Salinity regimen transition process.

986

987   The salinity condition within the estuary consists of a series of transitions from one
988   quasi-equilibrium condition to another. This concept was reflected in the LSMM program. The
989   program calculates the potential target (equilibrium) salinity based on the amount of freshwater
990   inflow. It then calculates the salinity change on daily time steps using the following equation:

991

992              $$SAL2 = SALEQ + (SAL1-SALEQ)*Exp(-cT)$$ [12]

993

994   where SAL1 is the salinity at the beginning of the time step, SAL2 is the salinity at the end of the
995   time step, SALEQ is the equilibrium salinity for certain amount of freshwater inflow after the
996   transition has completed. T is time and c is a constant that determines the speed of transition.
997   Apparently at the beginning of the time step (T=0), SAL2 = SAL1 and if the freshwater inflow
998   remains the same, SAL2 will eventually reach SALEQ.

999   Because the freshwater inflow is provided by the watershed model (WaSh) in daily time
1000 steps, the calculation of the Long-Term Salinity Management Model is carried at fixed time steps
1001 of 24 hours. The predicted salinity depends on both target (equilibrium) salinity and the initial
1002 salinity condition at the beginning of the time step. If the amount of freshwater inflow changes
1003 before the transition is completed, then a new transition begins and the program repeats the same
1004 computational procedure under the new flow condition.

1005 The LSMM is designed to assess daily average salinity over a long period of time. Because
1006 the program operates on daily time steps (versus minutes or seconds of a full hydrodynamic
1007 model), it allows the assessment of long-term data (39 years in this model simulation) at
1008 minimum cost and computing time. In addition to using hydrologic data provided by the WaSh
1009 model, the LSMM can also modify the hydrograph based on certain operational rules such as
1010 MFL criteria. The model also calculates the amount of freshwater demand for salinity
1011 management and nutrient loadings assuming a target concentration for inflows.

1012 **Figures 12-24** through **12-27** depict the salinity calculations of the LSMM. The output was
1013 compared with real data from four salinity stations in the Northwest Fork and the embayment
1014 area near the Jupiter Inlet. **Table 12-11** lists the statistical characteristics of both model prediction
1015 and field data. Statistics of the entire period of 517 days shows that the mean salinity of model
1016 output is slightly higher than field data at the four stations by 0.1 to 0.6 ppt. This is probably
1017 because the flow gauges on the Northwest Fork and major tributaries did not control 100 percent
1018 of the fresh water entering the system. **Tables 12-12** and **12-13** list the statistics of model
1019 prediction and field data for two relatively dry periods (March through May) and the rest of the
1020 year, respectively. In general, the simulated daily salinity matches well with the observed
1021 salinities statistically.

1022

1023

1024   **Table 12-11.** Comparison of statistical characteristics of model and field data.

Station Name	PD		BD		KC		RM9	
Date Type	Model	Field	Model	Field	Model	Field	Model	Field
Maximum	34.7	35.5	21.8	20.2	7.6	7.6	2.9	4.4
Minimum	25.0	22.4	1.1	0.2	0.1	0.1	0.0	0.1
Mean Value	32.1	31.8	11.1	9.7	2.1	1.5	0.6	0.5
Median Value	33.1	32.4	12.5	10.1	1.8	0.7	0.4	0.3
Standard Deviation	2.40	2.50	6.22	5.49	1.94	1.71	0.62	0.58
Data Count	517	477	517	502	517	506	517	199
Number of Missing Records	0	40	0	15	0	11	0	318

1025

1026

1027   **Table 12-12.** Comparison of statistical characteristics of model and field data –
        March through May.

1028

Station Name	PD		BD		KC		RM9	
Date Type	Model	Field	Model	Field	Model	Field	Model	Field
Maximum	34.7	35.5	21.8	20.2	7.6	7.6	2.9	4.4
Minimum	26.2	30.1	3.4	0.3	0.5	0.2	0.2	0.3
Mean Value	33.5	33.7	15.9	12.3	3.6	2.5	1.0	1.0
Median Value	33.8	33.9	15.9	13.1	3.1	1.7	0.7	0.5
Standard Deviation	1.40	1.19	3.98	4.97	2.04	2.08	0.78	0.87
Data Count	153	117	153	150	153	153	153	61
Number of Missing Records	0	36	0	3	0	0	0	92

1029

1030

1031

1032

1033   **Table 12-13.** Comparison of statistical characteristics of model and field data –
        June through February.

1034

Station Name	PD		BD		KC		RM9	
Date Type	Model	Field	Model	Field	Model	Field	Model	Field
Maximum	34.5	35.1	20.3	19.6	6.0	6.9	2.0	0.8
Minimum	25.0	22.4	1.1	0.2	0.1	0.1	0.0	0.1
Mean Value	31.5	31.1	9.1	8.6	1.5	1.1	0.4	0.3
Median Value	32.2	31.7	7.9	8.6	0.7	0.3	0.2	0.3
Standard Deviation	2.48	2.48	5.90	5.34	1.52	1.32	0.41	0.10
Data Count	364	360	364	352	364	353	364	138
Number of Missing Records	0	4	0	12	0	11	0	226

Salinity at River Mile 9.1, Northwest Fork Loxahatchee River
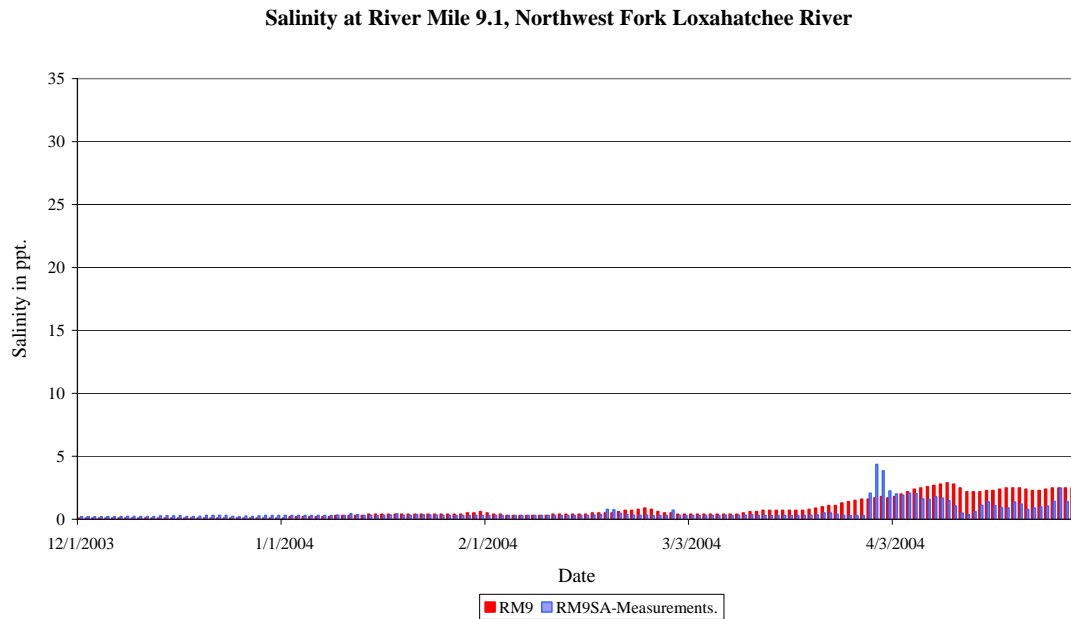
Figure 12-24. Field measurements versus salinity computation results for RM 9.12.

Salinity at Kitching Creek, Northwest Fork Loxahatchee River
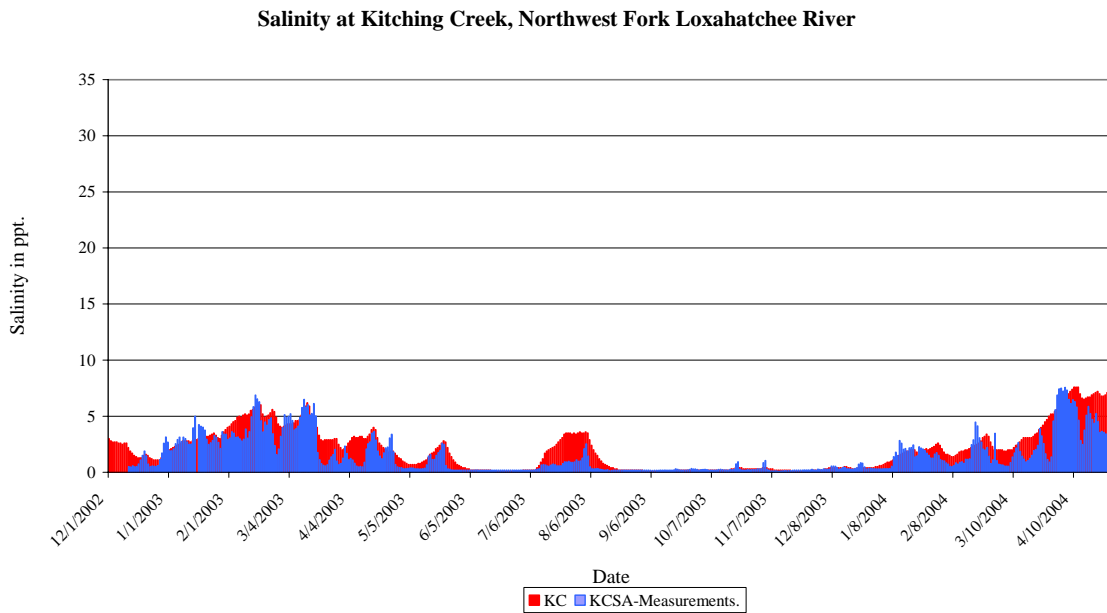
Figure 12-25. Field measurements versus salinity computation results for Kitching Creek (RM 8.13).

Salinity at Boy Scout Camp, Northwest Fork Loxahatchee River
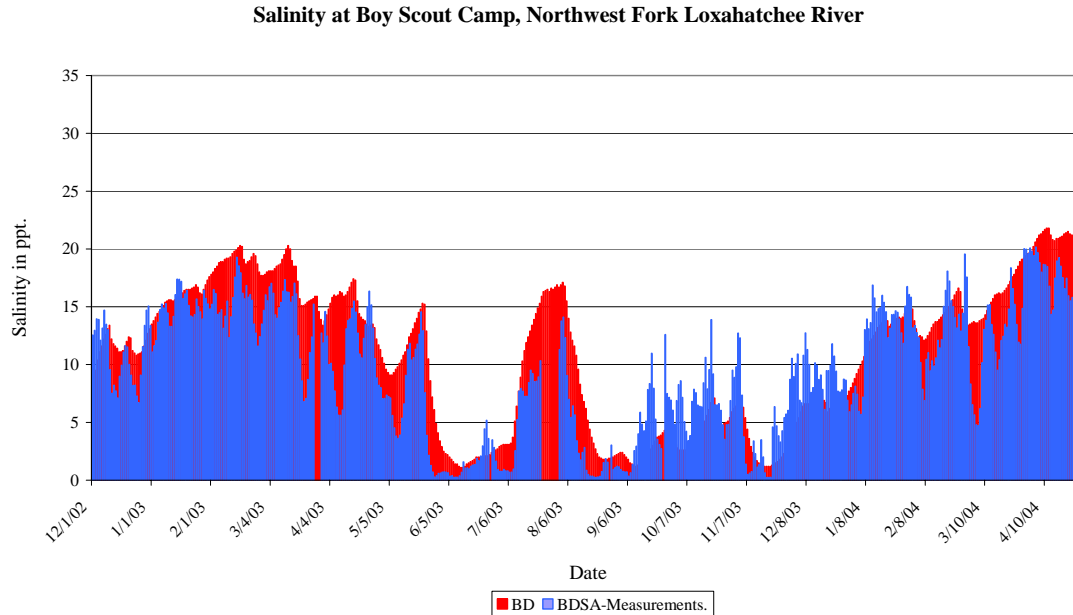
Figure 12-26. Field measurements versus salinity computation results
for Boy Scout Dock (RM 5.92).

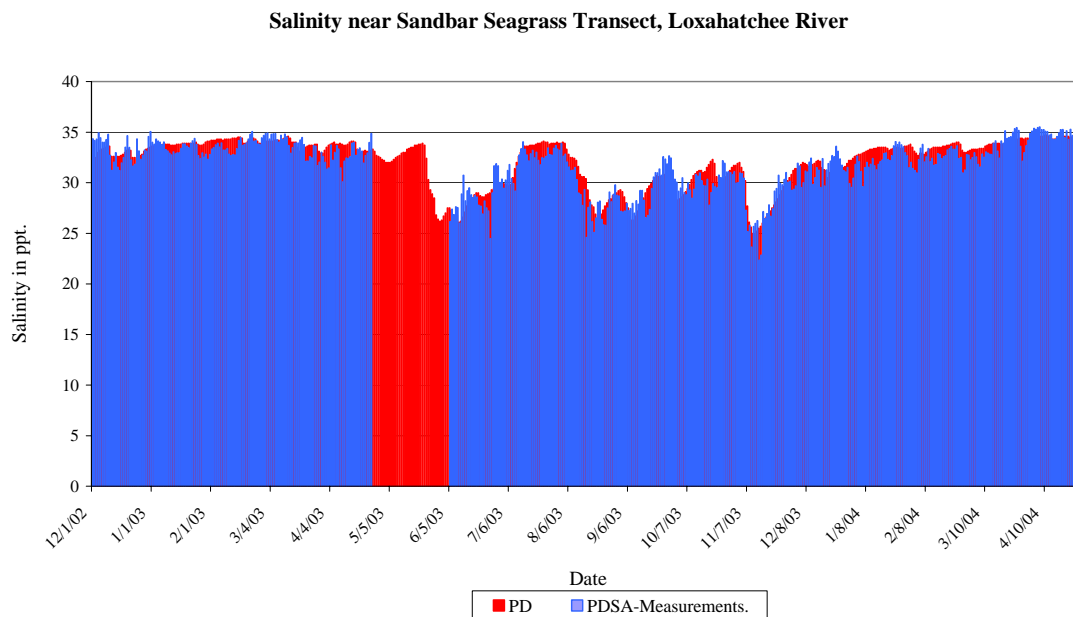**Salinity near Sandbar Seagrass Transect, Loxahatchee River**

Figure 12-27. Field measurements versus salinity computation results
for Pompano Drive Embayment Area (RM 1.77).

1035

MODELING THE NORTHWEST FORK ECOSYSTEM RESTORATION SCENARIOS

1036
1037

1038   The modeling results of the Loxahatchee WaSh model for the POR from 1965–2003 were
1039 used to establish the base project condition for scenario evaluation of Northwest Fork ecosystem
1040 restoration. The BASE simulation represents the existing or current conditions with no
1041 modifications. Five additional simulations were conducted with certain modifications to the
1042 BASE simulation hydrographs. The modifications represent scenarios that provide additional
1043 freshwater flows to upper Northwest Fork at Lainhart Dam and tributaries (Cypress Creek, Hobe
1044 Grove, and Kitching Creek) to reduce salinity in the freshwater segments of the Northwest Fork.
1045 The five restoration flow scenarios were designed to represent different levels of flows from a
1046 tributary or a combination of tributaries to the Northwest Fork. The scenarios were selected based
1047 on information provided by members of the public and agency representatives at meetings held to
1048 discuss the restoration of the Northwest Fork. For example, a flow of 65 cfs had been used as a
1049 flow target in the model for the development of the Northern Palm Beach County Comprehensive
1050 Water Management Plan (SFWMD, 2002b). **Table 12-15** summarizes the flow component(s) of
1051 each scenario. The LSMM was then used to predict daily salinity under the five scenario
1052 conditions at 15 locations (**Figure 12-16**). The simulated flow and salinity results were used to
1053 evaluate the ecological benefit with respect to each of the ecological components in the
1054 Northwest Fork.

1055   **Table 12-16** presents the salinity gradient of each scenario for the 15 study sites. Salinity
1056 ranges from near ocean conditions at the U.S. Coast Guard Station (RM 0.70; CG) near Jupiter
1057 Inlet to freshwater conditions at RM 9.12 in the Northwest Fork of the Loxahatchee River. The
1058 five scenarios that increase freshwater flows also lower the salinity throughout the river and the
1059 estuary.

1060   It is important to point out that the salinity condition in the Northwest Fork is extremely
1061 sensitive to the amount of freshwater inflow. A small change in freshwater flow of less than
1062 10 cfs can cause changes in salinity as high as several ppt in the upper Northwest Fork.
1063 **Table 12-16** only provides the average salinity for each site. Ecological evaluation of these
1064 scenarios is based on an analysis of daily salinity for the POR.

1065

1066

1067   **Table 12-15.** Long-Term Salinity Management Model simulation of
1068   restoration scenarios.

Scenario	Base Condition Hydrograph	Added Flows From Lainhart Dam	Added Flows From Tributaries	Total Added Flows	Approximate 2 ppt Saltwater Front Position
Base	1965-2003 base condition generated by watershed model	No additional flows	No additional flows	No additional flows from Lainhart Dam or tributaries	RM 9.5
LD65	1965-2003 base condition generated by watershed model	Water added as needed so flow is a minimum of 65 cfs at all times	No additional flows	Additional flows only from Lainhart Dam for a minimum of 65 cfs; No additional flows from tributaries	RM 8.5
LD65TB65	1965-2003 base condition generated by watershed model	Water added as needed so flow is a minimum of 65 cfs at all times	Water added as needed so flow is a minimum of 65 cfs at all times	Additional flows from Lainhart Dam and tributaries. Total flow is a minimum of 130 cfs at all times.	RM 8.0
LD90TB110	1965-2003 base condition generated by watershed model	Water added as needed so flow is a minimum of 90 cfs at all times	Water added as needed so flow is a minimum of 110 cfs at all times	Additional flows from Lainhart Dam and tributaries. Total flow is a minimum of 200 cfs at all times	RM 7.5
LD200	1965-2003 base condition generated by watershed model	Water added as needed so flow is a minimum of 200 cfs at all times	No additional flows	Additional flows only from Lainhart Dam for a minimum of 200 cfs; No additional flows from tributaries	RM 7.0
LD200TB200	1965-2003 base condition generated by watershed model	Water added as needed so flow is a minimum of 200 cfs at all times	Water added as needed so flow is a minimum of 200 cfs at all times	Additional flows from Lainhart Dam and tributaries. Total flow is a minimum of 400 cfs at all times	RM 6.0

1069

1070

1071   **Table 12-16.** Average salinity (ppt) at 15 study sites over the 39-year

1072   simulation period.

Salinity Study Site		Restoration Scenarios					
Site ID	River Mile	BASE	LD65	LD65TB65	LD90TB110	LD200	LD200TB200
CG	0.70	33.0	32.8	32.6	32.2	31.8	30.7
SGNB	1.48	32.0	31.6	31.3	30.4	29.6	27.6
SGSB	1.74	31.3	30.8	30.3	29.3	28.4	26.0
PD	1.77	31.2	30.6	30.2	29.2	28.3	25.8
SGPP	2.44	29.2	28.5	27.9	26.5	25.2	22.0
O1	2.70	26.9	26.1	25.4	23.7	22.3	18.7
O2	3.26	24.6	23.5	22.5	20.4	18.7	14.5
O3	3.74	22.5	21.0	19.9	17.4	15.5	11.0
O4	4.13	21.0	19.4	18.1	15.4	13.4	8.9
O5	4.93	16.2	13.9	12.2	9.1	7.2	3.5
O6	5.45	13.5	10.7	8.9	5.9	4.3	1.6
BD	5.92	10.9	7.9	6.2	3.7	2.5	0.7
VT9	7.06	5.8	3.0	1.8	0.7	0.4	0.2
KC	8.13	2.7	0.8	0.4	0.2	0.1	0.1
RM9	9.12	1.0	0.2	0.1	0.1	0.1	0.1

1073   **LITERATURE CITED**

1074   AQUA TERRA Consultants. 1998. Addition of Irrigation Module to the HSPH Model. Final
1075   Report submitted to South Florida Water Management District, West Palm Beach, FL.

1076   AQUA TERRA Consultants. 1996. Modifications to HSPF for High Water Table and Wetland
1077   Conditions in South Florida, Final Report submitted to South Florida Water Management
1078   District, West Palm Beach, FL.

1079   ASCE Task Committee on Definition of Criteria for Evaluation of Watershed Models of the
1080   Watershed Management Committee, Irrigation and Drainage Division. 1993. Criteria for
1081   Evaluation of Watershed Models. *Journal of Irrigation and Drainage Engineering*, 119(3):
1082   429-442.

1083   Donigian, A.S., J.C. Imoff, B.R. Bicknell and J.L. Kittle. 1984. Application Guide for
1084   Hydrological Simulation Program – FORTRAN (HSPF). EPA-600/3-84-065. U.S.
1085   Environmental Protection Agency, Athens, GA.

1086   FDEP. 1998. Loxahatchee River Watershed Action Plan. Second Draft. Florida Department of
1087   Environmental Protection, Tallahassee, FL.

1088   Hu, G. 2004. Modeling Study of Saltwater Intrusion in Loxahatchee River, Florida. In:
1089   *Proceedings of the 8th International Conference on Estuarine and Coastal Modeling*.
1090   In print, American Society of Civil Engineers, 2004.

1091   Hu, G. 2002. The Effects of Freshwater Inflow, Inlet Conveyance and Sea Level Rise on the
1092   Salinity Regime in the Loxahatchee Estuary. Proceedings of 2002 Environmental
1093   Engineering Conference, Environmental & Water Resources Institute, American Society of
1094   Civil Engineers-Canadian Society of Civil Engineers, Niagara Falls, Ontario, Canada,
1095   July 21-24, 2002.

1096   MacCready, P. 2004. Toward a Unified Theory of Tidally-Averaged Estuarine Salinity Structure.
1097   *Estuaries*, 27(4): 561-570.

1098   Russell, G.M. and B.F. McPherson. 1984. Freshwater Runoff and Salinity Distribution in the
1099   Loxahatchee Estuary, Southeastern Florida, 1980-82. USGS Water Resources Investigation
1100   Report 83-4244.

1101   Sculley, S. 1995. West Palm Beach Water Catchment Area Water Conservation Study Technical
1102   Memorandum No.2 Water Budget Model. Final Report (under Contract No. C-6113)
1103   submitted to the South Florida Water Management District, West Palm Beach, FL.

1104   SFWMD. 2002a. Technical Documentation to Support Development of Minimum Flows and
1105   Levels for the Northwest Fork of the Loxahatchee River. South Florida Water Management
1106   District, West Palm Beach, FL.

1107   SFWMD. 2002b. Northern Palm Beach County Comprehensive Water Management Plan
1108   Planning Document: Volume I. South Florida Water Management District, West Palm Beach,
1109   FL.

1110   USACE. 1996. Users' Guide to RMA2 Version 4.3. U.S. Army Corps of Engineers, Waterways
1111   Experiment Station, Hydraulic Laboratory.

1112   Wan, Y., C. Reed and E. Roaza. 2003. Modeling Watersheds with High Groundwater Tables and
1113   Dense Drainage Canals. p. 10. In: *Proceedings of 2003 AWRA International Congress:*
1114   *Watershed Management for Water Supply*, June 29–July 2, 2003, New York, NY.